Final Report

Crude Oil Viscosity Research and Dispersant Effectiveness Measurements

Paul D. Panetta, Jennifer Jerding, Alexandria Podolski, Hualong Du, and Richard Byrne

Applied Research Associates, Inc.

Report for

U.S. Department of the Interior
Bureau of Safety and Environmental Enforcement (BSEE)
Sterling, VA

August 2018

This study was funded by the Bureau of Safety and Environmental Enforcement (BSEE), U.S. Department of the Interior, Washington, D.C., under Contract Number E17PD00017.

ACKNOWLEDGMENTS

The authors wish to thank Edith Holder and Robyn Conmy for helpful discussions regarding the baffled flask test.

DISCLAIMER

This final report has been reviewed by the Bureau of Safety and Environmental Enforcement (BSEE). The findings and conclusions in this report are those of the author(s) and do not necessarily represent the views of the funding agency.

Table of Contents

EXECUTIVE SUMMARY

Oil spills in marine environments create a unique hazard for the environment and its inhabitants. When a spill occurs, responders—whose aim is to do the least damage to the environment while mitigating the spill—are faced with a series of choices. Alternative treatment methods with chemical agents, such as dispersants, are an important part of the mitigation effort to decrease the spread and impact from surface and subsurface releases. The main effect of dispersants on oil is to lower the surface tension at the oil-water interface so that the oil can break up into small droplets that may remain in the water column long enough to potentially be consumed by naturally occurring bacteria. It has been found that droplets with a diameter less than ~70 μm tend to stay in the water column due to natural turbulence [1]. Because of the large volume of dispersant used during spill responses like Deepwater Horizon, where 1.84 million gallons of chemical dispersants were used, it is important to know the efficiency of these agents so that they are not over-applied or under-applied to remove the most oil possible. It is also important to know the efficiency of dispersants on various oils to achieve an accurate calculation of the oil budget. The goal of this work was to determine the relationship between the dispersant effectiveness (DE) and the oil properties including viscosity and the concentration of saturates, aromatics, resins, and asphaltenes (SARA) in the oil.

To determine these relationships, the effectiveness of Corexit® 9500A and Finasol® to disperse nine different oils at 5°C and 20°C was studied using the baffled flask test (BFT). The kinematic viscosity of these oils ranged in from 23 cSt to 15,592 cSt. In addition to the baffled flask measurements of DE, the effectiveness of the DE was also measured using the Laser In-situ Scattering Transmissometry (LISST) instrument to measure the droplet size distribution directly. Measurements of the acoustic scattering from the oil-water mixtures were also studied to help advance that technology for potential use as a tool to measure dispersant effectiveness. The measurements of DE using the LISST was important because the LISST is the primary means that DE is measured in simulated environments such as meso-scale wave tanks and in the open water. The results from this project allowed for the direct comparison of DE using both techniques.

While the dispersant effectiveness is related to oil viscosity, the correlation was at most R^2 of 0.83, implying there could be other components in the oil that also affect the DE. Out of the two dispersants tested, Finasol generally has a higher DE than Corexit 9500A, and the relationship between viscosity and DE is slightly stronger. The data shows that the correlation between viscosity and DE for Corexit 9500A at 20ºC is significantly stronger than at 5ºC. The opposite relationship is observed for Finasol—the correlation between viscosity and DE for Corexit 9500A at 20ºC is weaker than at 5ºC. For both dispersants, DE is generally higher at 20ºC, which is expected because viscosities are lower at higher temperatures.

Asphaltenes show the highest correlation with DE with R^2 values of 0.4009 and 0.4448 for 20ºC and 5ºC, respectively, in which a higher R^2 value indicated a better fit (with a value of 1 being a perfect fit). Saturates have the weakest correlation with DE with R^2 values of 0.02 and 0.1 for 20ºC and 5ºC, respectively. DE of Finasol correlates with

asphaltenes the strongest with R^2 values of 0.2 and 0.4 for 20ºC and 5ºC, respectively. Saturates are also the most weakly correlated with DE of Finasol with R^2 values of 0.06 and 0.1 for 20ºC and 5ºC, respectively. Across all four hydrocarbon groups for both dispersants, the correlation was always stronger at 5ºC than at 20ºC.

One of the important conclusions that can be drawn from this study is that measurements of DE using the BFT and the LISST are very different with the LISST producing much smaller DE values. While the trends are the same, the differences were as much as a factor of 1.7 at 20°C and a factor of 27 at 5°C. The large differences between the LISST and the BFT could be related to the fact that they are measuring two distinctly different properties of the dispersed oil. In the BFT, the DE is determined based on the amount of oil that is in the water-oil mixture, while the LISST measurement of the DE[1] is determined as the percentage of oil with droplet sizes below 74.5 μm. The droplet size distributions had a significant number of droplets in the water-oil mixture with sizes above 74.5 μm. In the BFT, all of this oil was measured (even larger droplets) as dispersed, which may be a cause for the disagreement in DE between the two methods.

The acoustic measurements of backscattering amplitude correlated strongly with DE at 20°C with a R^2 value of 0.97 but less so at 5°C with a R^2 value of 0.3. The amplitude of the backscattering also correlated strongly with the d_{30} (the droplet size that corresponds to 30% of the droplets) with an R^2 value of 0.8 at 20°C. The frequency response of the backscattering did not correlate strongly with the DE or average droplet size for the oils measured.

For future measurements, it is recommended that the DE be correlated with additional properties of the oil, such as those measured using Gas Chromatography/Mass Spectrometry (GC/MS) tools. It is also recommended that DE measurements be performed at Ohmsett or at a similar meso-scale tank to determine the effects of the larger, more realistic scale and mixing energy to the open water than can be achieved in the tank. As part of that work at Ohmsett, it would be valuable to directly compare LISST results with the results from liquid-liquid extraction followed by UV-Visible (UV-Vis) measurements on the same samples from the Ohmsett tank so that any variations between LISST- and BFT measurements can be studied and understood. It is also recommended that acoustic measurements be performed, and an appropriate theory that can accommodate an arbitrary size distribution be used.

The results from this work provide useful information about the amount of oil dispersed in the water column. Future work at Ohmsett is recommended to provide data in a relevant environment to potentially increase the accuracy of the oil budget for future spills.

1 The LISST reports the particle size distribution in bins with a spacing based on the size of the detecting ring. For this instrument, the particle sizes near 70 μm are 63.5 μm and 74.5 μm. Since the detector did not provide a spacing of exactly 70 μm, we chose 74.5 μm because it was closer to 70 μm than the next smaller ring.

1. OVERVIEW AND OBJECTIVE

Oil spills in marine environments create a unique hazard for the environment and its inhabitants. When a spill occurs, the responders—whose aim is to do the least damage to the environment while mitigating the spill—are faced with a series of choices. Alternative treatment methods with chemical agents, such as dispersants, are an important part of the mitigation effort to decrease the spread and impact from surface and subsurface releases. Dispersants have been used to treat many oil spills, like the Deepwater Horizon incident where 1.84 million gallons of chemical dispersants were used, including 771,000 gallons injected at the wellhead. The main effect of dispersants on oil is to lower the surface tension at the oil-water interface and thus, decrease the size of the oil droplet. The resultant smaller droplets may then remain in the water column when driven by natural turbulence, long enough to potentially be consumed by naturally occurring bacteria. It has been found that droplets with a diameter less than ~70 μm tend to stay in the water column due to natural turbulence [1]. A schematic of this process and a photo of dispersants applied to a surface slick at Ohmsett are shown in Figure 1.

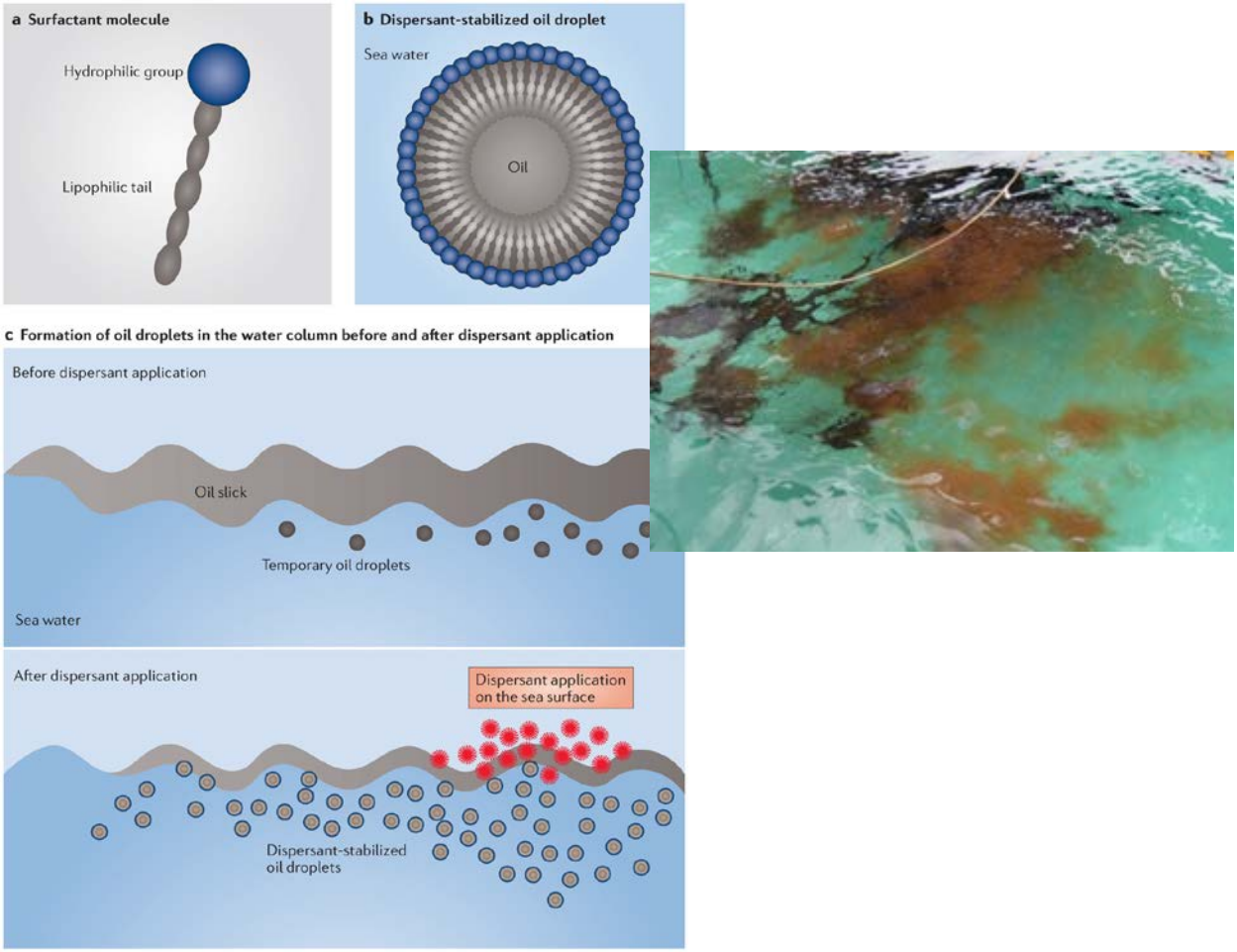

Figure 1. Schematic of dispersant action, courtesy of Nature Reviews-micro (left), and a photograph of dispersant effects on oil at Ohmsett (right).

The dispersant effectiveness (DE) is a measure of how well the dispersant breaks up and stabilizes the oil into the water column. In laboratory environments, the DE is determined using a swirling or baffled flask test (BFT); dispersant is applied to the oil slick, mixed, and the concentration of oil in a sample taken from the water column is measured using gas chromatography or UV-Visible (UV-Vis) spectrophotometry. In the open water and in wave tanks, DE is determined by measuring the percentage of below 70 μm using Laser In-Situ Scattering Transmissometry (LISST).

There are many factors that control the effectiveness of the dispersants, including the formulation and application method of the dispersant, the mixing energy of the water, its temperature and salinity, the oil properties (including viscosity), chemical composition, and the degree of weathering and emulsification. Many researchers have shown that the ability to disperse oil is directly related to the viscosity [2] of the oil. One recent example from a study conducted by Holder is shown in Figure 2, where DE was measured using the BFT and plotted versus kinematic viscosity of oil. The data shows the dispersant effectiveness generally increases as viscosity decreases. A closer look at the data shows a large spread at low viscosity ranging from about 45% to almost 90% for kinematic viscosities[2] below 2500 cSt. To determine the effects of oil viscosity and composition, the DE was measured for oils ranging in kinematic viscosity from 12 cSt to 3376 cSt. This large spread implies that other factors are important to consider, such as chemical composition. Thus, the SARA composition was also measured to provide additional information about how or if other oil properties affect the DE.

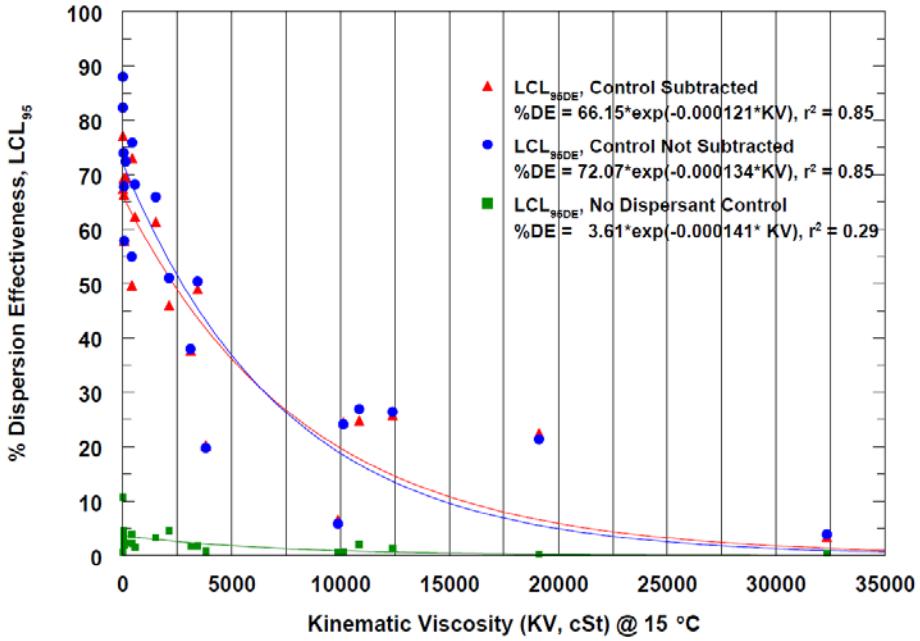

Figure 2. Dispersant effectiveness versus kinematic viscosity from the BFT [3].

2 Kinematic viscosity (units of cSt) is calculated by dividing dynamic viscosity (units of cP) by density (g/mL).

Directly relating the DE at lab scales using the BFT and larger scales at Ohmsett and the open water is difficult at best, as can be seen in Figure 3, where the correlation between BFT and measurements at Ohmsett and the Warren Springs Laboratory are shown. The agreement is very poor between the DE measured with the BFT and the measurements at Ohmsett with measurements of the DE using the BFT near 25% and the DE at Ohmsett ranging as high as 100%. The mixing modality in the lab and the open water are quite different, but so are the methods of measuring dispersant effectiveness. In the lab, Holder used a UV/Vis spectrophotometer to measure the concentration of oil dispersed in a sample taken from the water column after mixing in a baffled flask [3]. In large-scale tanks and in open water, the effectiveness is determined by the decrease in oil droplet size measured ~1 m below the surface of the water using a LISST and benchmarked with the amount of oil collected from the surface of the water. Note that oil droplets with a diameter less than 70 µm tend to remain suspended in the water column [4]. To help shed light on the reason for these differences, DE was measured in our study (using the BFT) and the oil droplet size was measured (using the LISST) on samples taken from the same baffled flask. As part of this study, the science base of acoustic measurements of droplet size was also advanced. Measuring the DE with a common measurement protocol between both the lab and the field will potentially allow results from the lab tests to be predictive for large-scale tanks and in open water.

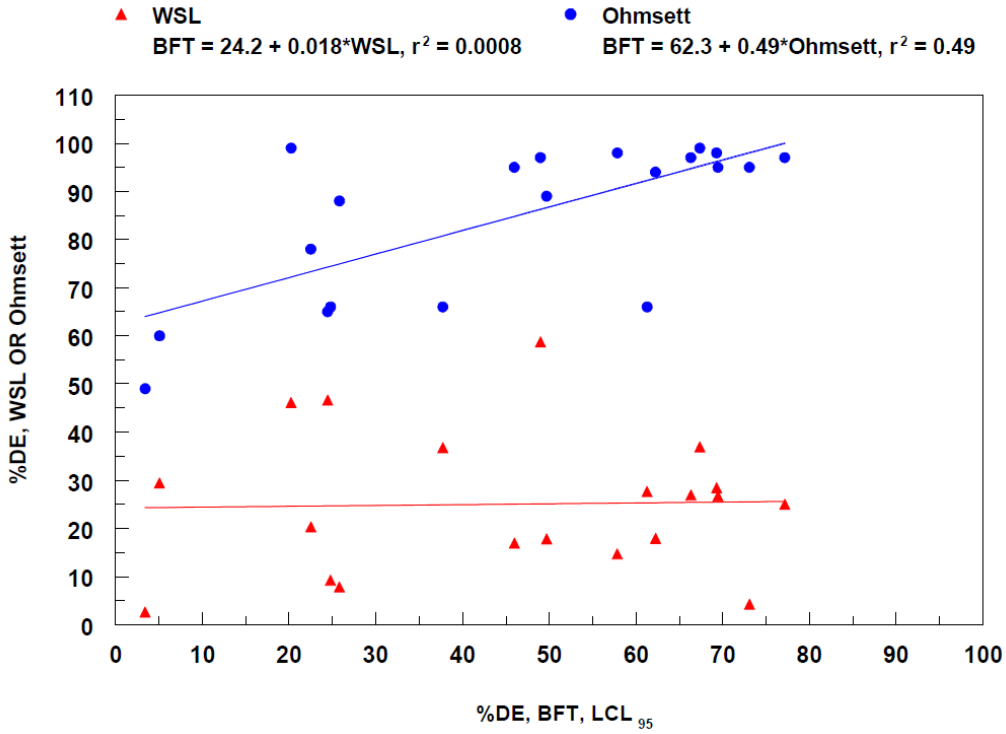

Figure 3. Dispersant effectiveness from the BFT correlated with dispersant measurements at Ohmsett and a second lab [3].

2. LITERATURE REVIEW, OIL PROPERTIES, AND TEST MATRIX

2.1. LITERATURE REVIEW

Dispersants were first used as an oil spill countermeasure on a large scale in 1967, when the Torrey Canyon supertanker spilled 120,000 tonnes of oil off the England coastline. Dispersants work as an oil spill countermeasure by breaking oil slicks into small oil droplets that can be dispersed into the water column, enhancing microbial degradation with natural occurring microbes given the increase surface area. The surfactants within dispersants have both a lipophilic, hydrocarbon-based tail and a hydrophilic, polar head group to form a layer at the oil-water interface. The lipophilic end orients within the oil and the hydrophilic end orients within the water. The objective of dispersants is to lower the interfacial tension between oil and water, and with wave action or mixing energy, to create oil droplets with a diameter less than 70 µm that will remain suspended in the water column rather than rise to the surface [4].

DE is generally defined as the degree to which the dispersant “works” or disperses oil into the water column [5]. DE is usually expressed as a percentage and is measured by a large array of testing methods both in the laboratory and on a larger scale. In the laboratory, the BFT has been adopted as the official method for evaluating oil spill dispersants and measuring DE, but other bench-scale methods include the Exxon Dispersant Effectiveness Test (EXDET) and the Swirling Flask Test (SFT), amongst others [3]. Large wave tanks are also used for full-scale testing of oil spill dispersants, such as the wave tank at the Ohmsett facility in Leonardo, New Jersey. A LISST particle size analyzer and in-situ fluorometer are used at Ohmsett to measure oil drop sizes and in-water oil concentrations, respectively [6]. DE can be calculated from the amount of oil left on the surface of the water versus total oil spilled [6], from observed changes in dispersed oil concentration within samples or determined from data on oil drop size distribution [7]. The correlation between DE results from bench-scale tests such as BFT and large-scale Ohmsett tests appears to be low [8]. Additional work should be performed to find better agreement between lab-scale and large-scale methods. Also, for each bench-scale test, the procedures differ and DE is defined and measured in a different way, which leads to varying results. The movement to using BFT as the official bench-scale dispersant test has improved the correlation and repeatability in test results conducted at different facilities [3].

There are many theories in the literature on the various factors that influence DE. One factor widely reported in the literature as influencing DE is oil viscosity. DE tends to be higher for less viscous oils than more viscous oils. Some researchers, such as Holder [8] and Belore [9], argue for a strong correlation between DE and oil viscosity, while other researchers argue for a more general correlation and emphasize that there are other parameters that strongly influence DE. Belore [9] conducted tests at Ohmsett and reported a maximum viscosity of 10,000 cP for effective dispersion and that dispersants were ineffective at viscosities beyond the maximum. Canaveri [10] tested oils with Corexit® using the EXDET method and found significant variability in DE (from 14% to 44%) for oils with viscosities around 5,000 cSt, suggesting more of a general trend between DE and viscosity.

Since increasing viscosity and decreasing DE is not a perfect trend, there are certainly other factors at work such as temperature, water salinity, mixing energy, oil density, oil chemistry, dispersant composition, and many more [5] [11]. Oil chemistry is complicated and varies widely from oil to oil. The components of oil are often broadly grouped into four categories: saturates, aromatics, resins, and asphaltenes (SARA). Many researchers have hypothesized that SARA composition can have a significant effect on DE and studies were performed to address this hypothesis.

In a dispersion study conducted by Mukherjee [11], where oil composition was systematically manipulated by varying the relative concentrations of SARA fractions and then performing the BFT, it was found that higher aromatic fractions created a statistically significant increase in DE. Mukherjee also found that DE increased when both saturates and resins existed in higher fractions. This study also looked at the possible influence of SARA on oil droplet size distribution with dispersants. Higher fractions of saturates favored small (<7 μm) to medium sized droplets (7 μm–20 μm). Interactions between saturates and asphaltenes also promoted small and medium-sized droplets, whereas interactions between aromatics and asphaltenes promoted larger-sized droplets (>20 μm).

Fingas [12] performed DE experiments using the SFT and found that oils with increased saturate content had higher DE, and oils with increased aromatic and asphaltenes content resulted in lower DE. This result differs from the Mukherjee study that found higher DE with increased aromatic content. Yet another study (Blondina [13]) found different results on the influence of aromatics depending on the dispersant used. DE was higher with higher fractions of aromatics when Corexit 9527 was used and either lower are very mildly higher when Corexit 9500 was used, but these dispersants only differ by solvent in their composition.

In the Canaveri EXDET tests mentioned above [10], increased saturate content was found to decrease DE—this is also in contrast to what Fingas [12] found. Due to the variability and seeming contradiction in how SARA content influences DE, it is evident that more research is needed in this area to either support or dispute prior results.

The temperature at which the experiments are performed is another key parameter that affects the effectiveness of dispersants. While DE experiments have been performed at a range of temperatures by researchers (e.g., BFT by Holder at 5°C, 15°C, and 25°C [3]), it is generally true that DE goes down as temperatures get colder. This behavior can be an indirect effect, meaning lower temperatures create higher oil viscosity, which in turn lowers DE; it could also impact the reaction of dispersant with oil as surfactants become more soluble in colder water [5]. Dispersants become more viscous with colder temperatures as well, which can limit the penetration and mixing of dispersants with oil. Also, as oil temperature increases, the interfacial tension between water and oil will decrease, which promotes dispersion.

2.1.1. Influence of Literature Review on Test Matrix

The above information from the literature is by no means an exhaustive summary on the factors that drive DE (paraffin/wax content was not mentioned, for example); these specific findings impacted the test matrix created for this project. The test matrix was designed to primarily look at three factors that impact DE: temperature, viscosity, and SARA content. As previously mentioned, research on how SARA content influences DE has produced variable results, and the industry can benefit from additional investigation with more oils and more dispersants to further clarify this subject. The test matrix was also designed to take a closer look at how viscosity impacts DE; it seems to be fairly well accepted that dispersants can be ineffective on extremely viscous oils, so ARA chose to concentrate mostly on crude oils with kinematic viscosity less than 15000 cSt at 5°C.

In addition, two temperatures were chosen for the test matrix to investigate temperature effects: 5°C and 20°C. This selection was primarily driven by the oil property testing that ARA had a third party perform—SARA content was evaluated and viscosity was measured at both 5°C and 20°C. Two dispersants were also chosen for test matrix—Corexit 9500A and Finasol®—as they are more heavily stockpiled for oil spill response around the globe [14].

2.2. OIL PROPERTIES

Crude oils can be categorized into light, medium, and heavy oils using either kinematic viscosity or the American Petroleum Institute (API) gravity—a relative measure of density. Crude classification using kinematic viscosity defines light oils as oils with viscosities between 10 cSt and 100 cSt, medium oils as oils with viscosities between 100 cSt and 500 cSt, and heavy oils as oils with viscosities greater than 500 cSt. The nine fresh oils used in this study were classified as three light oils, two medium oils, and four heavy oils at 20ºC using kinematic viscosity (see Table 1). API classification defines light crudes with an API gravity greater than 31.1, a medium crude with an API gravity between 22.3 and 31.1, and a heavy crude with an API gravity below 22.3 [15]. This study chose to focus on crude classification using kinematic viscosity rather than API gravity due to the perceived influence viscosity may have on DE.

The density of the oils used in the study was determined using ASTM 5002, and the dynamic viscosity was determined using ASTM D7042, which is accurate for lighter oils up to 500 cP. Density and dynamic viscosity were measured for each oil at 5°C and 20°C. The measured values at 20°C are shown in Table 1.

Table 1. Oil viscosity and density from laboratory analysis.*

Oil Name	Dynamic Viscosity @ 20°C, cP	Viscosity Kinematic @ 20°C, cSt	Density @ 20°C, g/ml	Density @ 60˚F g/mL	API Gravity @ 60˚F	Viscosity Classification	API Classficiation
Anadarko	11	12	0.916	0.919	22.5	light	medium
ANS (fresh)	25	29	0.874	0.876	30.0	light	medium
Ewing Bank	29	32	0.897	0.903	25.1	light	medium
Endicott	256	276	0.929	0.932	20.3	medium	heavy
Alpine	317	345	0.918	0.919	22.5	medium	medium
IFO 120	1035	1085	0.954	0.955	16.7	heavy	heavy
Doba Chad	1657	1791	0.925	0.929	20.9	heavy	heavy
Rock	2617	2723	0.961	0.965	15.2	heavy	heavy
Platform Gina (fresh)	3244	3376	0.961	0.965	15.2	heavy	heavy

*Kinematic viscosity (units of cSt) was calculated by dividing dynamic viscosity (units of cP) by density (g/mL), not measured directly. Kinematic viscosity values listed in brown are from calculations.

The viscosity versus density for these oils (shown in Figure 4) generally follows the typical relationship for crude oil—those with higher viscosity have a higher density. The data points at 5°C have a higher viscosity than those at 20°C for the same density. The lines shown in the plot are arbitrary trend lines to point out the interesting outlier, which is Anadarko crude. This oil sample was tested to have an unusually high density to viscosity ratio, which may be useful in separating which property is the driver for some dispersant-oil interactions.

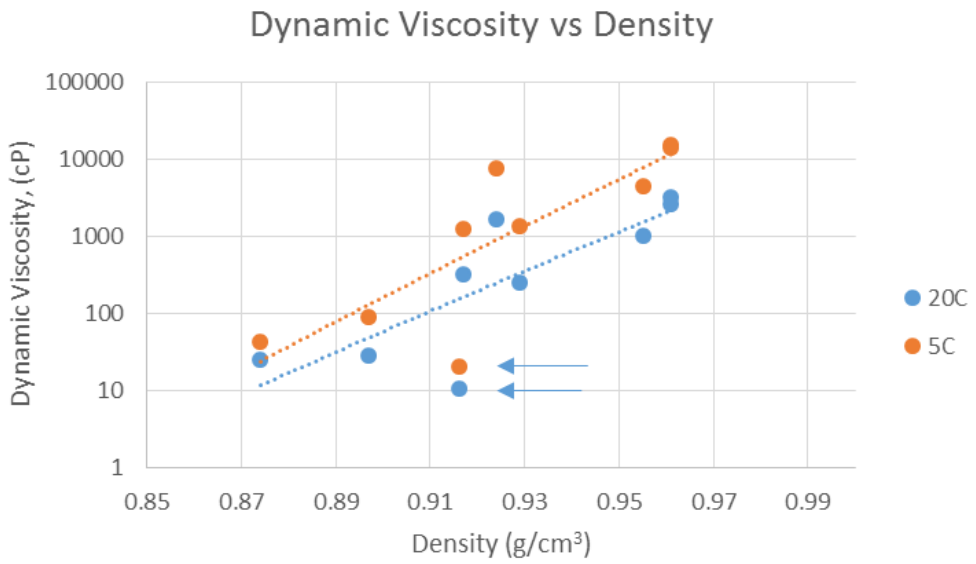

Figure 4. Dynamic viscosity versus density for oils in the study. Arrows show Anadarko as an outlier.

The oil samples were tested for SARA composition using a Iatroscan TLC-FID (thin layer chromatography and flame ionization detector) according to standard method IP-469. The IP-469 method determines all four compound classes by adsorption chromatography (which in the case of asphaltenes, may under-predict by 20% especially for the lighter oils) [16]. Retaining the oil samples and evaluating the methodology and results in this ongoing study using a more accurate test for asphaltenes, such as IP-143,

may be valuable. The breakdown of SARA components for the nine oils are shown in Table 2.

Table 2. SARA components of laboratory tested oils.

Oil Name	Viscosity Kinematic@ 20^{0}C, cSt	Saturates % m/m	Aromatics % m/m	Resins (Polar I) % m/m	Asphaltenes (Polar II) % m/m	Sulfur Content wt %
Anadarko	12	58.00	40.30	1.70	0.10	0.23
ANS (fresh)	29	44.50	41.20	13.30	1.00	0.65
Ewing Bank	32	27.2	52.3	14.4	6.1	1.36
Endicott	276	50.00	33.70	14.30	6.00	0.15
Alpine	345	29.40	47.30	14.70	8.60	1.62
IFO 120	1085	24.70	51.40	18.90	5.00	2.44
Doba Chad	1791	22.90	44.90	23.10	9.10	0.95
Rock	2723	13.70	43.70	24.00	18.60	3.64
Platform Gina (fresh)	3376	14.30	39.30	23.60	22.80	4.06

The dominant identified driver on dispersant effectiveness is viscosity and/or density, since they are highly correlated. The SARA components were measured to help determine if viscosity dominantly controls dispersant effectiveness or if one or more of the SARA components are primary or secondary factors that contribute to dispersant effectiveness.

A few key observations are below:

- For the light and medium crude oils:
  - Alpine has high saturates relative to its viscosity.
  - Alpine has low resins and low asphaltenes.
  - Anadarko has a high density:viscosity ratio.
- For the heavy oils:
  - Doba Chad has high saturates relative to its position in the viscosity order.
  - Platform Gina (fresh) and Rock Crude have very close SARA components.

2.2.1. Weathering

While not a primary component of this study, the difference in DE between fresh Alaskan North Slope (ANS) crude oil and weathered ANS was also measured. Evaporative weathering was performed on a sample of ANS to achieve an overall mass loss of 21% over the course of six hours. Perforated polyethylene tubing with holes connected to an air compressor diffused the sample of ANS with air at 5 psi, as shown in Figure 5. Mass measurements, as well as oil temperature measurements, were recorded hourly until the desired mass loss was achieved. To mitigate fumes, the evaporative weathering took place inside an enclosed, ventilated apparatus.

Figure 5. Evaporative weathering set up for ANS.

The weathered sample of ANS could not be tested for viscosity/SARA, so approximate values were determined based on trends extrapolated from values published by Environment Canada in the Environmental Technology Centre Oil Properties database [17].

2.3. TEST MATRIX

This study used two commercially available dispersants, Corexit 9500A and Finasol. Both of these dispersants are part of the Global Dispersant Stockpile (GDS), which is made up of dispersants with the widest worldwide approvals, as well as the Environmental Protection Agency (EPA) National Contingency Plan (NCP) list, which controls what can be used in U.S. waters. Corexit 9500A is the primary dispersant stockpiled in the United States with 132,000 gallons stored in Fort Lauderdale, Florida, while a total of 835,750 gallons of Finasol is stocked throughout the United Kingdom, Singapore, France, and South Africa. With both Corexit 9500A and Finasol making up a majority of the GDS, they are likely to be considered for use in actual spill events. [14]

The study used nine fresh oils and one weathered oil (10 total oils), ranging from light to heavy crudes with a variety of SARA compositions. Some oils, like ANS, are commonly found in literature and were chosen in order to directly compare to previous studies. Other oils, like Platform Gina (fresh), are less commonly found in literature and were chosen to supplement existing data.

Viscosity changes dramatically with temperature, so each oil-dispersant combination was tested at both 5ºC and 20ºC to span a wider range of viscosities. Measuring dispersant effectiveness at two temperatures also indicated a temperature dependent chemical reaction between the oil and dispersant. Table 3 shows the complete test matrix.

Table 3. Completed test matrix for baffled flask test, LISST, and acoustic measurements.

	Dispersant Effectiveness - BFT				Dispersant Effectiveness - LISST				Dispersant Effectiveness - Acoustics			
	20°C		5°C		20°C		5°C		20°C		5°C	
Crude Oil	Corexit 9500A	Finasol	Corexit 9500A	Finasol	Corexit 9500A	Finasol	Corexit 9500A	Finasol	Corexit 9500A	Finasol	Corexit 9500A	Finasol
Anadarko	✓	✓	✓	✓								
ANS (fresh)	✓	✓	✓	✓	✓		✓		✓		✓	
ANS (weathered)	✓	✓	✓	✓	✓		✓		✓		✓	
Ewing Bank	✓	✓	✓	✓								
Endicott	✓	✓	✓	✓								
Alpine	✓	✓	✓	✓	✓		✓		✓		✓	
IFO 120	✓	✓	✓	✓								
DOBA (CHAD)	✓	✓	✓	✓	✓		✓		✓		✓	
Rock Crude	✓	✓	✓	✓								
Platform Gina (Fresh)	✓	✓	✓	✓	✓	✓	✓	✓	✓	✓	✓	✓

3. BAFFLED FLASK TEST

In order to determine DE of Corexit 9500A and Finasol for 10 different crude oils at two temperatures, the same general approach and procedure for the BFT outlined by Holder [3] was used and is reported here. The protocol uses a 150-mL screw-cap trypsinizing flask (essentially an Erlenmeyer flask with baffles) that has been modified by the placement of a glass stopcock near its bottom so that a subsurface water sample can be removed without disturbing the surface oil layer, as shown in Figure 6.

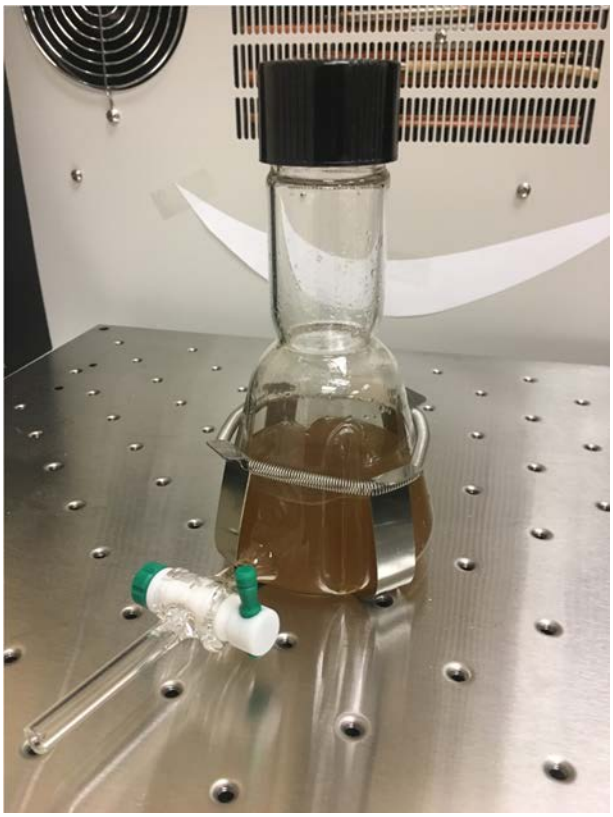

Figure 6. Baffled Trypsinizing Flask allows for subsurface extraction of dispersed oil.

After synthetic seawater and oil are added to the flask, a dispersant is added directly to the floating oil slick, and the flask is placed on a MaxQ-4000 orbital shaker table to receive moderate turbulent mixing at 200 rpm for 10 ± 0.5 min. The shaker table having a speed control unit with variable speed (15–500 rpm) and an orbital diameter of approximately 0.75 inches (1.9 cm) is used to impart turbulence to solutions in the test flasks. The mixing is equivalent to an energy dissipation rate of 0.163 W/kg water (or m^2/s^3) [18], which is approximately two orders of magnitude greater than that obtainable in the Swirling Flask Test. The rotational speed accuracy should be within ± 10%. The contents are allowed to settle for 10 ± 0.25 minutes to allow non-dispersed oil to return to the water surface, as shown in Figure 7, before removing the subsurface water sample. Each test is run individually by the same analyst for each dispersant-oil combination so that identical test conditions can be maintained for each set of tests.

Figure 7. IFO120 slick reformation after 10-minute settling time.

The subsurface water sample is then processed by liquid-liquid extraction in dichloromethane (DCM). A Unico SQ-3802 UV-Vis spectrophotometer is used to measure the absorbance of the sample at 340 nm, 370 nm, and 400 nm. The absorbance values of the extract are then compared against a calibration curve to determine the oil concentration of the extract. The calibration curve is derived from the absorbance measurements of six solutions of known concentration created from a single stock solution made up of the oil-dispersant combo under test (see Section 3.3 on the Oil Standards Procedure).

Four tests for each dispersant-oil combination were performed at both test temperatures. Tests were performed with and without dispersant in order to account for natural dispersion. The calibration curves required 180 extractions to account for six concentration levels, the ten oils, and three dispersant conditions (Corexit 9500A, Finasol, and None). Four method blanks were also prepared to confirm proper quality control.

3.1. SYNTHETIC SEAWATER

Synthetic seawater was created by dissolving 34 g of Instant Ocean in 1 L of Milli-Q water (34 ppt final salinity).

3.2. BAFFLED FLASK PROCEDURE

Each dispersant-oil-temperature combination test was replicated four times. The Grubbs' test [19] was used to identify any outliers, in which case the outlying replicate was replaced with an additional replicate. The only exception is the Platform Gina (Fresh) Replicate Three (R3) at 20ºC, which was not replaced with another replicate due to unavailability of the LISST to reanalyze oil droplet size.

For this work, the BFT was performed using the following procedure:

Add 120 mL of synthetic seawater to the baffled flask. Bring seawater to target experiment temperature (either 5°C+0/-1°C or 20°C+0/-1°C) and place flask into temperature controlled orbital shaker[3], shown in Figure 8. Carefully dispense 100 µL of oil directly onto the surface of the synthetic seawater using an Eppendorf Repeater pipettor. Dispense 4 µL of dispersant onto the center of the oil slick, making certain the dispersant contacts the oil before the water. Shake the flask for 10 minutes at a rotational speed of 200 rpm using the orbital shaker. At the end of the mixing period, prior to sampling, allow the flask to remain stationary in the orbital shaker for 10 minutes—temperature is maintained to ±1°C during shaking and settling time. Remove flask and immediately drain 2 mL and discard. Immediately collect a 30-mL sample. Transfer the 30-mL sample to a 125-mL separatory funnel and perform liquid-liquid extraction three times with 5 mL fresh DCM to extract dispersed oil from the seawater—collect extracted oil/DCM solution in 50-mL graduated cylinder. Adjust the extract to a final volume of 20 mL and transfer to a vial with sealed top and store at 5°C until the time of analysis. Certain extracts were diluted with an additional 20 mL of DCM before analysis to stay within the absorbance measurement range of the Unico SQ-3802 UV-Vis Spectrophotometer (Figure 9).

The current ASTM standard method for laboratory oil spill dispersant effectiveness using the baffled flask somewhat differs from the procedure outlined above. The standard dictates that oil and dispersant should be premixed before being placed on water, opposed to placing oil followed by dispersant. For the purpose of this study, placing dispersant directly on a floating oil slick more closely mimicked an in-situ oil spill scenario

[3] Orbital shaker already set to target test temperature and allowed time to equilibrate to that temperature.

and was directly comparable to the work of Holder. The standard uses gas chromatograph to analyze extracts, instead of UV-Vis measurements. In order for the results from this study to be directly comparable to the previous studies, UV-Vis measurements were preferable. The standard does not take natural dispersion into account when reporting dispersant effectiveness. It is highly recommended that future adaptations to the current standard should take natural dispersion into consideration. The overall ability of an oil to be dispersed includes both the chemical effect of the dispersant and the physical effect of breaking wave motion, taken into account by natural dispersion.

Examples of replicate samples at the two test temperatures and their relative color difference (a visible indication of oil concentration in the sample) are shown in Figure 10. Color difference for the same oil tested at two different temperatures seemed to depend on viscosity in many cases; higher viscosity oils were lighter at the colder temperature indicating that less oil was dispersed.

Figure 8. ThermoScientific MaxQ 4000 Orbital Shaker has an enclosed, temperature controlled chamber to minimize temperature fluctuations during testing.

Figure 9. Unico UV-Vis Spectrophotometer used to make absorbance measurements.

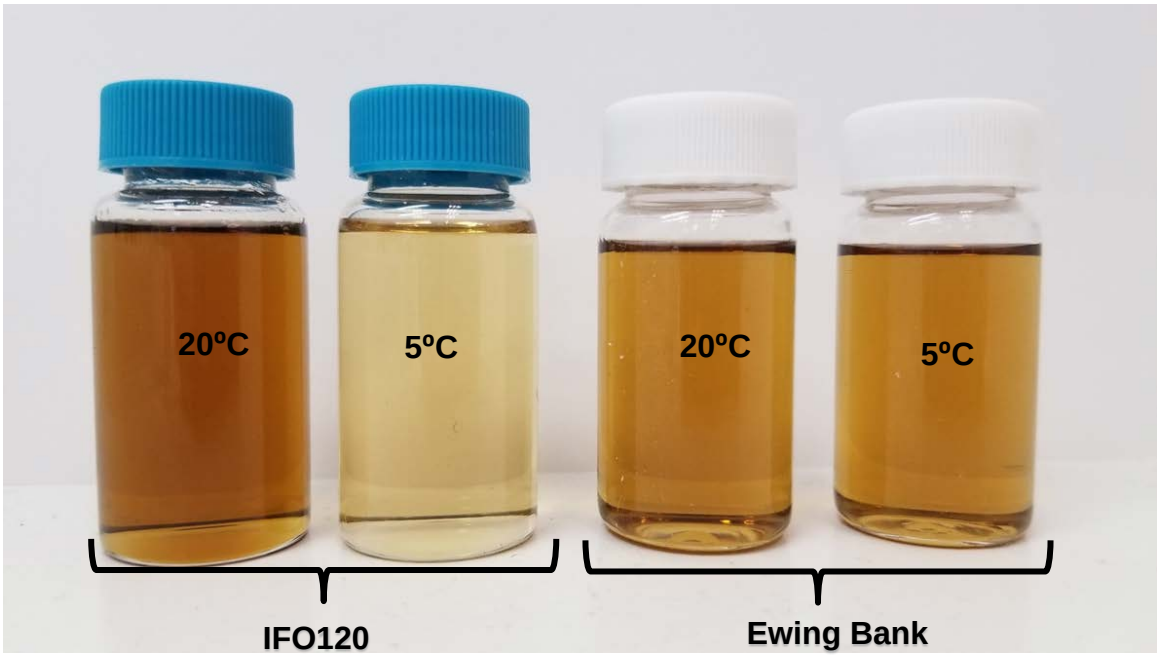

Figure 10. (Left to Right): IFO120: 20^0C, IFO120: 5^0C, Ewing Bank: 20^0C, Ewing Bank: 5^0C. After adjusting the volume to 20 mL following liquid-liquid extraction, the color difference between higher viscosity samples, like IFO120, can be significant, while the color difference between lower viscosity samples, like Ewing Bank, is much closer.

3.3. Oil Standards Procedure and Calibration Curve Generation

For every oil-dispersant combination tested, a stock solution of dispersant-oil mixture in DCM was prepared by first adding 18 mL of DCM to a vial, followed by 2 mL of oil and

finally 80 µL of the dispersant. Stock solution concentrations were based on the oil density (measured in the lab from room temperature oil samples) and volumes of each addition. Stock solutions were also created without dispersant for each oil in the study to compare against test replicates without dispersant (natural dispersion tests).

For generating a six-point calibration curve, specific volumes of the stock standard solution were added to 30 mL synthetic seawater in a 125-mL separatory funnel and then extracted three times with 5 mL DCM to collect six calibration samples. Typically, the volumes of the stock solution added to the separatory funnel for the six calibration samples were 20, 50, 100, 150, 200, and 300 µL as depicted in Figure 13; however, for some calibration curves for oils without dispersants, the volumes of the stock solution were 5, 10, 20, 50, 100, and 150 µL.

To create a six-point calibration curve, the six calibration samples were analyzed using the UV-Vis to measure absorbance at 340 nm, 370 nm, and 400 nm. The absorbance values for each wavelength are then plotted, and the area under the absorbance versus wavelength curve is calculated using the trapezoidal rule (Figure 11). The calculated area is then plotted against oil concentration for each of the six calibration samples. A linear trendline is added to the data (with a y-intercept of zero) and the slope of this trendline (calibration curve slope) is then used to calculate oil concentration in the test replicates. The data analysis process is discussed in Section 3.4.

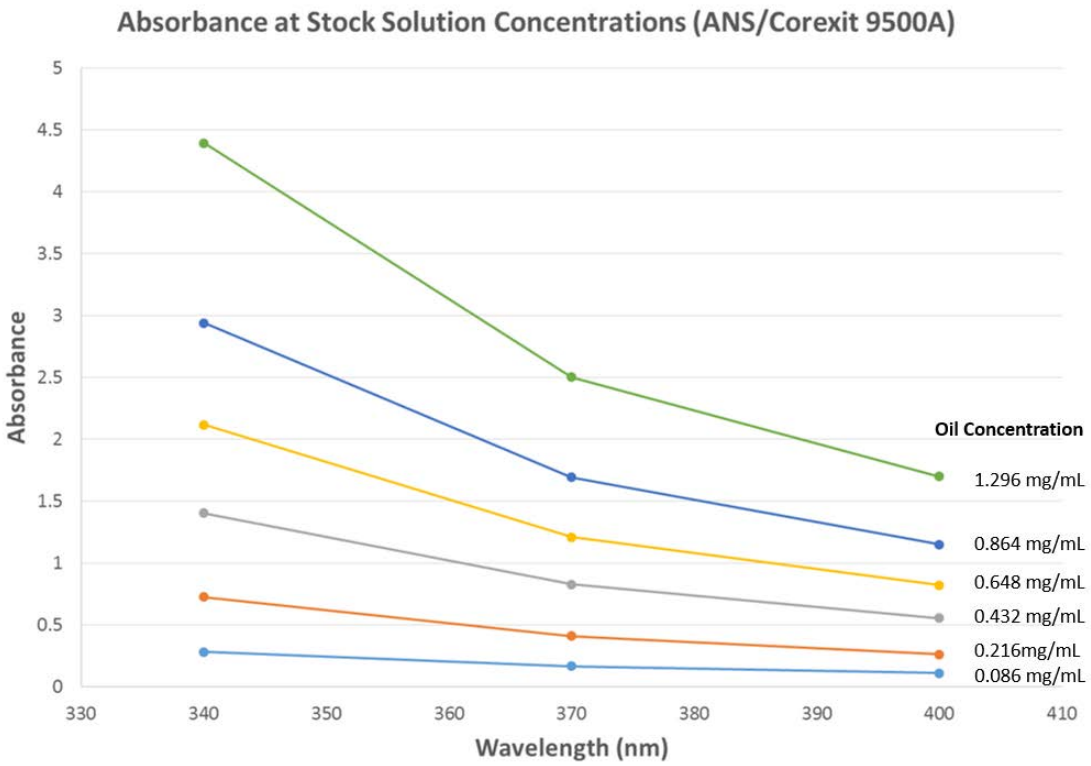

Figure 11. The concentration curve for each calibration sample is created by plotting the measured absorbance at 340 nm, 370 nm, and 400 nm. The trapezoidal rule, Equation 1, is then used to measure the area under each concentration curve. Each area is then plotted as a function of concentration.

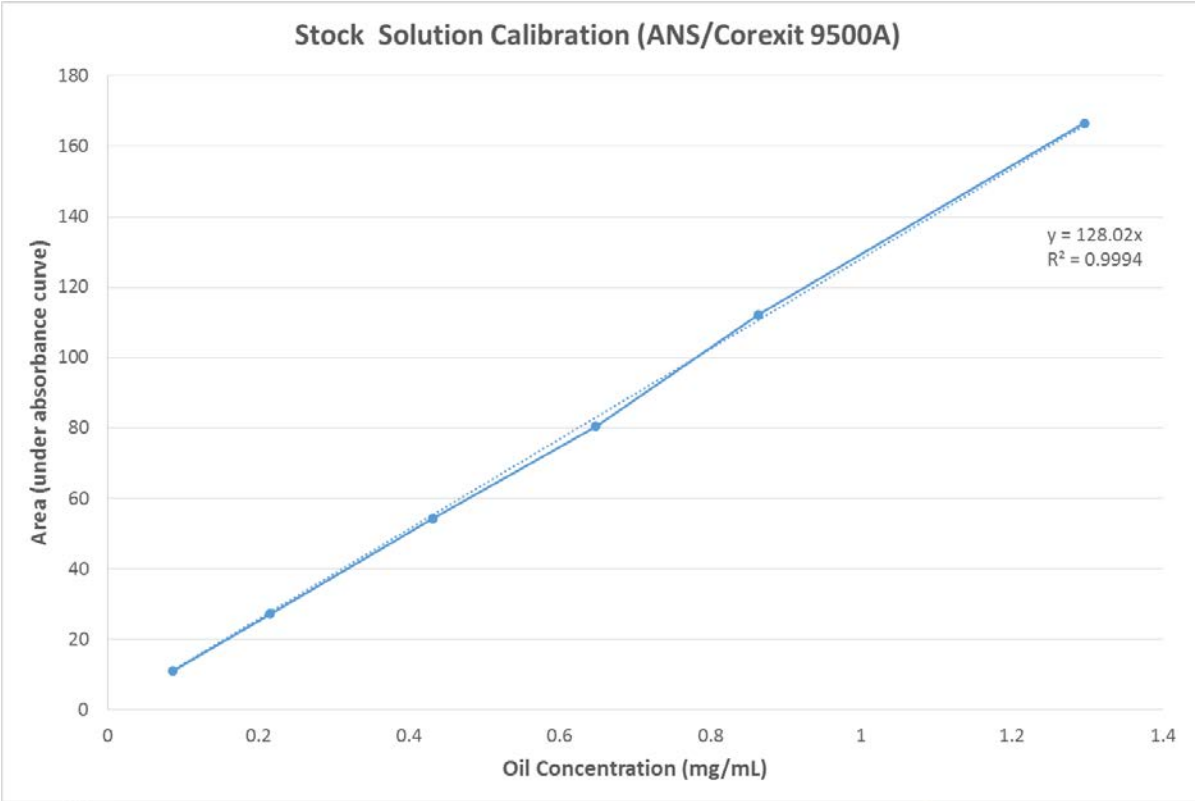

Figure 12. The calibration curve is the linear trend line fit to the oil concentration versus area under the calibration curve. It should be noted that this linear trend line has a fixed y-intercept at 0; this is because when taking UV-Vis measurements, the machine measures all samples against a DCM blank.

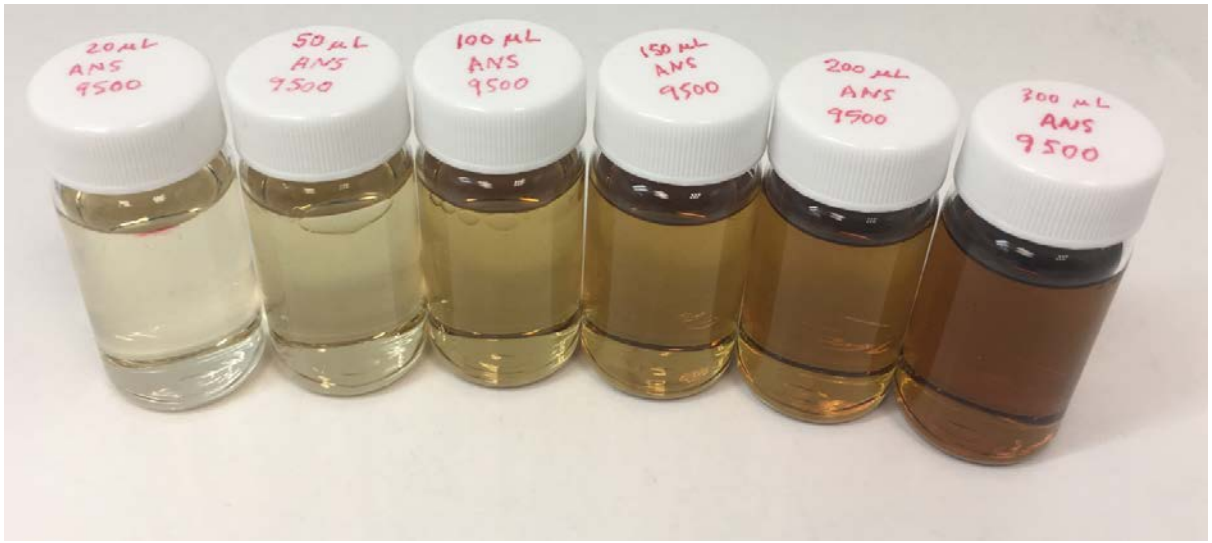

Figure 13. The absorbance of samples with known concentrations of ANS is measured and used to create a calibration curve to calculate the oil concentrations for samples with unknown concentrations.

3.4. Data Analysis Process

The data analysis procedure outlined by Holder [3] was followed during this study to calculate DE. Absorbance was measured for each test replicate using the UV-Vis.

The absorbance at three discreet wavelengths of 340, 370, and 400 nm was recorded, and the area under the absorbance versus wavelength curve was calculated by applying the trapezoidal rule according to the following equation:

$$Area = \frac{Abs_{340}+Abs_{370}\times 30}{2} + \frac{Abs_{370}+Abs_{400}\times 30}{2} \quad (1)$$

This area count was used to calculate the Total Oil Dispersed and then the percentage of oil dispersed (%OD) based on the ratio of oil dispersed in the test system to the total oil added to the system, as follows:

$$TotalOilDispersed(g) = \frac{Area}{CalibrationCurveSlope} \times V_{DCM} \times \frac{V_{tw}}{V_{ew}} \quad (2)$$

The dispersion effectiveness value calculated is the lower 95% confidence level of the four independent replicates. Equation 5 summarizes the calculation of the LCL_{95}:

where:

V_{DCM} = volume of DCM extract,
V_{tw} = total volume of seawater in flask,
V_{ew} = total volume of seawater extracted, and

$$\%OD = \frac{TotalOilDispersed}{\rho_{oil}\times V_{oil}} \quad (3)$$

where:
ρ_{oil} = density of the specific test oil, $\frac{g}{L}$, and
V_{oil} = volume(L)of oil added to test flask ($100\mu L = 10^{-4}$ L) (4)

$$LCL_{95} = \bar{x} - t_{n-1,1-\alpha}\left(\frac{s}{\sqrt{n}}\right) \quad (5)$$

where $\bar{x}$ = mean dispersion effectiveness of the $n = 4$ replicates
s = standard deviation, and
$t_{n-1,1-\alpha} = 100 \times (1-\alpha)^{th}$ percentile from the $t-$ distribution with $n - 1$ degrees of freedom
For four replicates, $t_{n-1,1-\alpha} = 2.35$, where $\alpha = 0.05$.

Since a certain amount of physical dispersion occurs when no dispersant is used, that fraction should be accounted for (i.e., subtracted) in the final reporting of chemical dispersion. The statistical equations governing the proper way to accomplish this are summarized below. The average nominal percent oil dispersed due to dispersant alone is calculated using Equation 6 for coupled experiments with and without dispersant ($\%OD_d$ and $\%OD_c$, respectively):

$$DE_{nom} = \overline{\%OD_d} - \overline{\%OD_c} \quad (6)$$

where:
DE_{nom} = nominal percent of oil dispersed due to dispersant alone,
$\overline{\%OD_d}$ = average % oil dispersed (total dispersed oil)
$\overline{\%OD_c}$ = average percent oil dispersed without dispersant

The same comparison for reporting the LCL_{95} is made for the coupled experiments with and without dispersant (LCL_{95d} and LCL_{95c}, respectively). The lower 95% confidence level (LCL_{95}) of the dispersion effectiveness (DE) or LCL_{95DE} is calculated after correcting for natural dispersion using the following equations:

$$LCL_{95DE} = \overline{\%OD_d} - \overline{\%OD_c} - (t_{n_d+n_c-2,0.95} * SE_{\bar{d}-\bar{c}}) \quad (7)$$

where:
LCL_{95DE} = lower confidence limit for dispersed oil due to dispersant only
$t_{n_d+n_c-2,0.95}$ = 1.94, the 95% critical value for a t-distribution with (n_d + n_c – 2) degrees of freedom.
$SE_{\bar{d}-\bar{c}}$ = standard error, defined in Equation 8:

$$SE_{\bar{d}-\bar{c}} = \sqrt{\frac{s_d^2}{n_d} + \frac{s_c^2}{n_c}} \quad (8)$$

LCL_{95DE} is the DE value reported.

3.5. BAFFLED FLASK TEST RESULTS

A total of 240 tests were performed. The dispersant-oil-temperature combinations are outlined in Table 4. Additionally, each oil-temperature combination was tested without a dispersant to account for natural dispersion.

Table 4. Baffled Flask Test matrix combinations

	20°C		5°C	
Oil	Corexit 9500 A	Finasol	Corexit 9500A	Finasol
Anadarko	✓	✓	✓	✓
ANS (fresh)	✓	✓	✓	✓
ANS (weathered)	✓	✓	✓	✓
Ewing Bank	✓	✓	✓	✓
Endicott	✓	✓	✓	✓
Alpine	✓	✓	✓	✓
IFO 120	✓	✓	✓	✓
Doba Chad	✓	✓	✓	✓
Rock	✓	✓	✓	✓
Platform Gina (fresh)	✓	✓	✓	✓

Some replicates had to be repeated due to being an outlier according to the Grubbs' test [20] or Maximum Normal Residual Test; however, this was infrequent. If an

outlier was detected by the Grubbs' test ($p<0.5$), then another replicate was run to replace the outlier.

Outliers tended to occur during naturally dispersed tests or cold tests. Outliers could have been resultant of droplets of oil gathering at the connection between the baffled flask and stopcock, as shown in Figure 14. Occasionally, while taking the 30-mL sample for liquid-liquid extraction, some of these droplets would become dislodged. Inclusion of these large droplets that were not truly dispersed may have caused samples to have larger oil concentrations, thereby falsely indicating a higher DE.

Figure 14. Droplets of ANS (fresh) gathering at connection between baffled flask and stopcock. These droplets occasionally became dislodged, causing the replicate to have a higher than average oil concentration, making it an outlier.

A separate but related issue of oil droplets sticking to glassware, as shown in Figure 15, was more common. While some small droplets of more viscous dispersed oil samples left a visible residue, most droplets sticking to the graduated cylinder were due to large droplets captured at the flask-stopcock interface that became dislodged. Since these large droplets often stuck to the graduated cylinder, they were prevented from skewing the sample, minimizing their impact. On occasion, too much residue left on the graduated cylinder may have caused an outlier with a sample lacking an oil concentration reflective of the replicate overall.

Figure 15. After sample was taken and poured into the separatory funnel, some large oil droplets remain on the graduated cylinder.

3.6. OVERALL DISPERSANT EFFECTIVENESS

The test matrix was designed to evaluate DE of two dispersants at two different temperatures for 10 oils. Each dispersant-temperature combination is isolated in order to evaluate changes in DE in response to these variables. The summarized results for all oil-dispersant-temperature combinations are tabulated and included in the Appendix.

"Average % Oil Dispersed ($\%OD_d$)" and "Std. Dev." Refer to the average and standard deviation of the four replicates for each oil-dispersant-temperature combination. Final DE was the lower 95% confidence limit for the nominally dispersed oil, which took naturally dispersed oil into account, across four replicates (LCL_{95DE}).

Table 5 and Figure 16 summarize the results from tests at 20ºC with Corexit 9500A. Both are organized by descending final DE. An oil is considered effectively dispersed if the final DE is above 75% [3]. With this criteria, Corexit 9500A would be a viable spill response for all tested oils except for Endicott, Rock, and Platform Gina (Fresh). The

standard deviation is under 5% for all oils except for Platform Gina (fresh) and Rock. The high standard deviations associated with these two oils could be due to their high viscosity.

Table 5. Dispersant effectiveness (DE) results for Corexit 9500A at 20C. Data is sorted in descending order by the final DE. Kinematic viscosity for ANS (weathered) is just an estimate based on weathering curves.

Oil	Kinematic Viscosity, cSt	Average % Oil Dispersed (%OD_d)	St. Dev.	Final Dispersant Effectiveness LCL_{95DE}	Crude Category by kinematic viscosity
ANS (fresh)	25	87.56%	2.31%	82.90%	medium
Ewing Bank	28.95	94.58%	4.02%	82.61%	medium
IFO 120	1035	84.36%	11.00%	80.17%	heavy
Alpine	317	89.54%	4.36%	79.21%	heavy
ANS (weathered)	60	86.99%	1.03%	78.71%	medium
Anadarko	10.57	94.07%	1.92%	78.71%	medium
Doba Chad	1657	81.59%	3.26%	74.96%	heavy
Platform Gina (fresh)	3244	76.75%	3.35%	72.60%	heavy
Endicott	256	77.23%	1.24%	72.13%	heavy
Rock	2617	74.27%	14.86%	58.99%	heavy

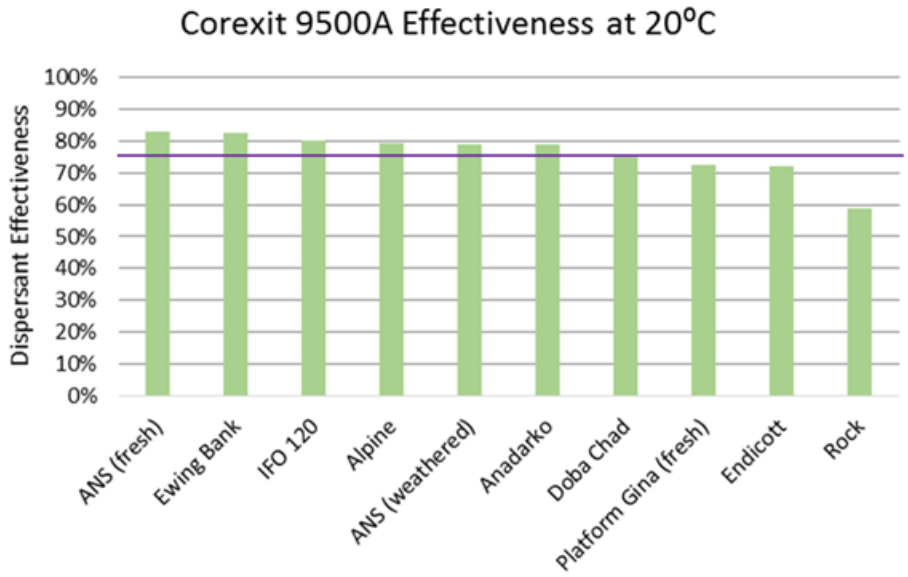

Figure 16. The effectiveness of Corexit 9500A at 20°C. Oils are listed in the order of highest DE to lowest DE, from left to right. All oils at or above 75% are considered effectively dispersed.

Table 6 summarizes the results from tests at 20ºC with Finasol. Both are organized by descending final DE. Similarly to the data set at 20ºC with Corexit 9500A, all but three oils are effectively dispersed. Endicott, an oil not effectively dispersed by Corexit 9500A, was the most effectively dispersed oil by Finasol. Also strikingly different is that despite

its low viscosity, weathered ANS was the least effectively dispersed oil. All standard deviations are below 4%.

Table 6. DE results for Finasol at 20ºC. Data is sorted in descending order by final DE. Kinematic viscosity for ANS (weathered) is just an estimate based on weathering curves.

Oil	Kinematic Viscosity, cSt	Average Oil Dispersed ($\%OD_d$)	St. Dev.	Final Dispersant Effectiveness LCL_{95DE}	Crude Category by kinematic viscosity
ANS (fresh)	25	88.51%	1.24%	84.77%	medium
Endicott	276	89.02%	1.78%	83.40%	heavy
Ewing Bank	43	91.98%	0.35%	83.20%	medium
Anadarko	12	95.45%	1.53%	80.28%	medium
Rock	2723	83.23%	3.45%	79.02%	heavy
Alpine	345	87.60%	3.39%	78.50%	heavy
IFO 120	1085	83.13%	3.75%	75.71%	heavy
Doba Chad	1791	79.22%	2.75%	73.08%	heavy
Platform Gina (fresh)	3376	68.95%	2.54%	65.68%	heavy
ANS (weathered)	60	44.71%	0.35%	36.81%	medium

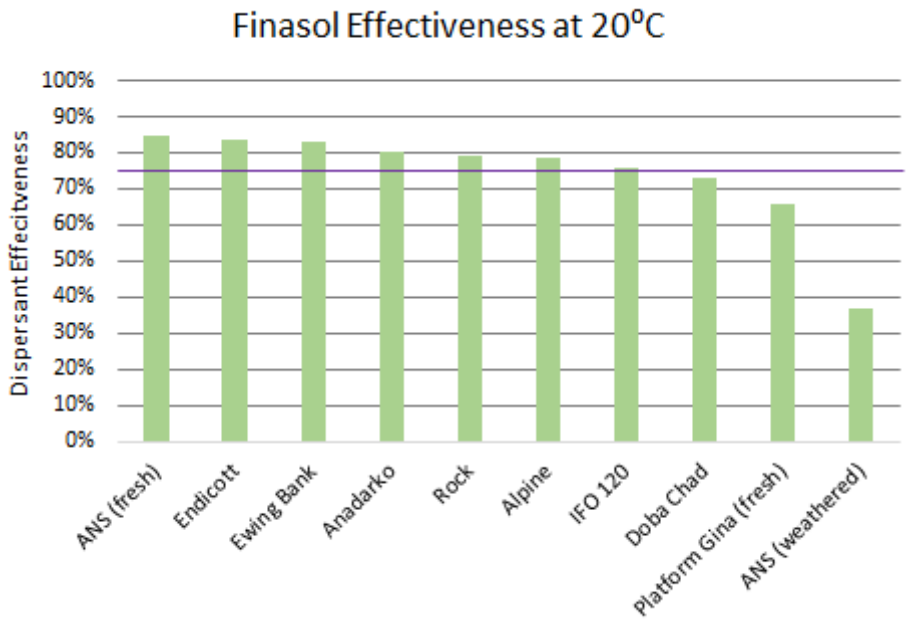

Figure 17. The effectiveness of Finasol at 20ºC. Oils are listed in the order of highest DE to lowest DE from left to right. All oils at or above 75% are considered effectively dispersed.

Table 7 and Figure 18 summarize the results from testing Corexit 9500A at 5ºC. Only five of the oils are effectively dispersed—the five oils with the lowest viscosity out of the test set. The standard deviation is generally pretty low, under 4%, except for a couple of high-viscosity oils, which still have standard deviations under 7%.

Table 7. DE results for Corexit 9500A at 5^{0}C. Data is sorted in descending order by final DE. Kinematic viscosity for ANS (weathered) is just an estimate based on weathering curves.

Oil	Kinematic Viscosity, cSt	Average Oil Dispersed (%OD_d)	St. Dev.	Final Dispersant Effectiveness LCL_{95DE}	Crude Category by kinematic viscosity
Ewing Bank	102	88.49%	1.03%	80.51%	heavy
ANS (fresh)	49	84.94%	2.45%	77.57%	medium
Anadarko	23	91.62%	1.46%	77.00%	medium
ANS (weathered)	90	81.37%	1.77%	74.49%	medium
Alpine	1368	80.78%	3.66%	67.46%	heavy
Endicott	1464	68.76%	2.93%	63.66%	heavy
Doba Chad	8321	32.84%	6.59%	23.54%	heavy
Platform Gina (fresh)	15592	25.45%	3.07%	22.16%	heavy
Rock	14593	23.47%	4.03%	19.21%	heavy
IFO 120	4690	18.58%	5.89%	12.11%	heavy

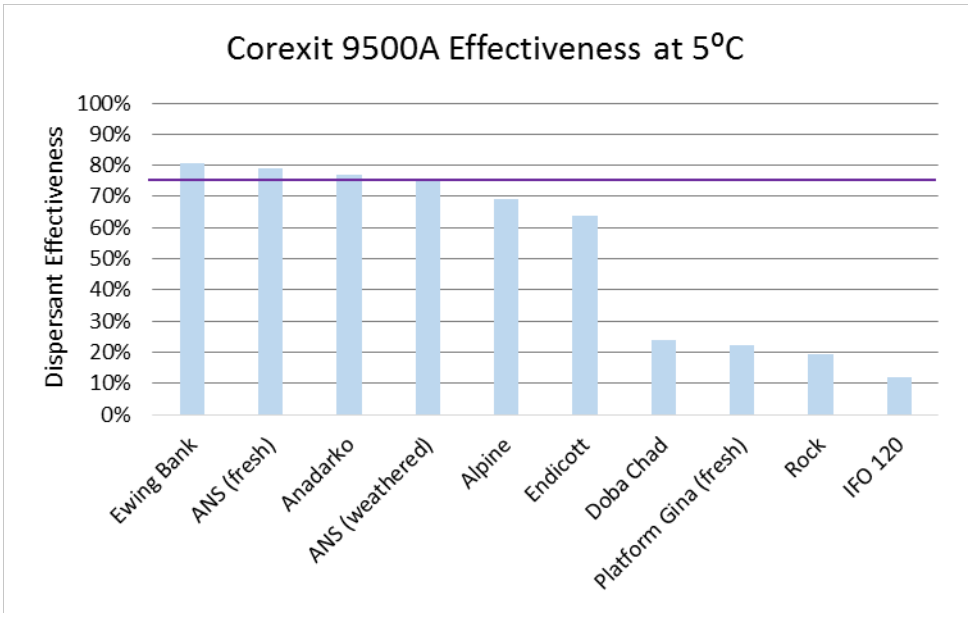

Figure 18. The effectiveness of Corexit 9500A at 5ºC. Oils are listed in the order of highest DE to lowest DE from left to right. All oils at or above 75% are considered effectively dispersed.

Table 8 and Figure 19 summarize the results of tests performed at 5ºC with Finasol, both of which are sorted in descending order by the final DE. Oil dispersion with Finasol at 5^{0}C follows the same general trend of oil dispersion with Corexit 9500A. Endicott was not effectively dispersed by Corexit 9500A, but effectively dispersed by Finasol at both 5ºC and 20ºC. Standard deviations for replicates with Finasol at 5ºC are generally under 5% except for two high viscosity oils, which still have standard deviations below 9%.

Table 8. DE results for Finasol at 5ºC. Data is sorted in descending order by final DE. Kinematic viscosity for ANS (weathered) is just an estimate based on weathering curves.

Oil	Kinematic Viscosity, cSt	Average % Oil Dispersed ($\%OD_d$)	St. Dev.	Final Dispersant Effectiveness LCL_{95DE}	Crude Category by kinematic viscosity
Anadarko	23	95.49%	0.75%	81.26%	medium
Ewing Bank	102	87.22%	1.29%	79.47%	heavy
Endicott	1464	83.88%	2.60%	79.10%	heavy
ANS (fresh)	49	85.20%	4.16%	76.33%	medium
Alpine	4690	83.87%	1.58%	72.52%	heavy
ANS (weathered)	90	42.24%	1.43%	35.63%	medium
Rock	14593	37.28%	4.23%	32.87%	heavy
IFO 120	4690	38.22%	7.06%	30.60%	heavy
Doba Chad	8321	28.10%	4.33%	21.10%	heavy
Platform Gina (fresh)	15592	24.60%	4.50%	19.95%	heavy

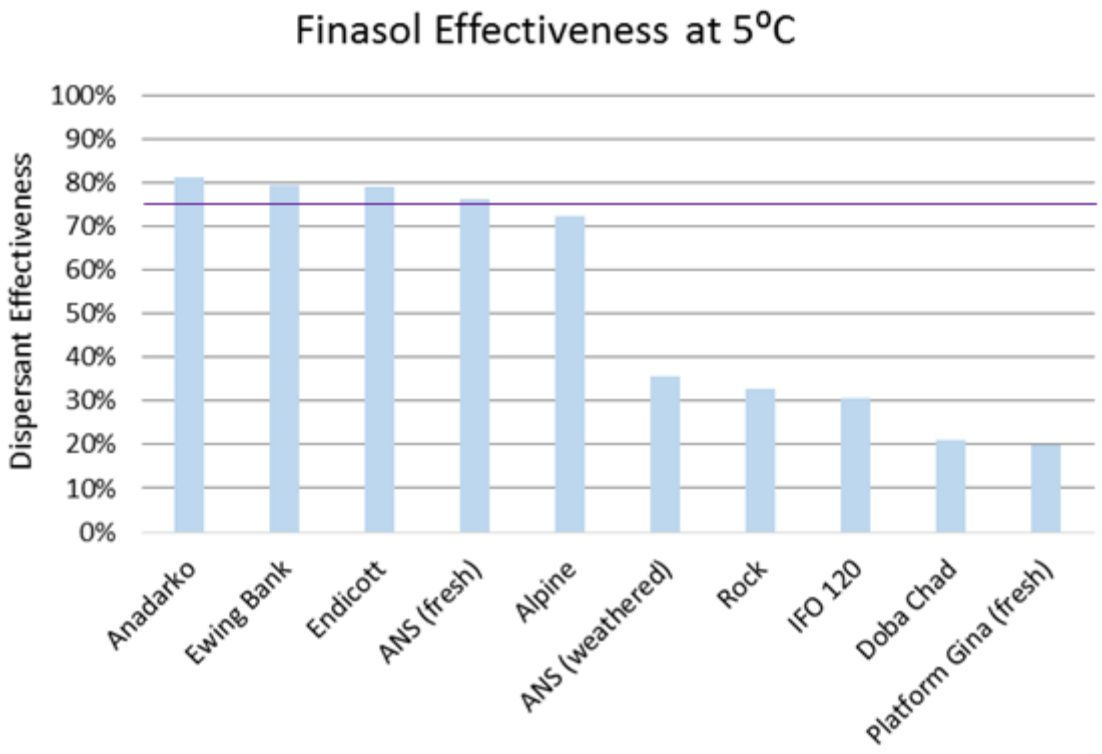

Figure 19. The effectiveness of Finasol at 5ºC. Oils are listed in the order of highest DE to lowest DE from left to right. All oils at or above 75% are considered effectively dispersed.

3.7. VISCOSITY AND DISPERSANT EFFECTIVENESS

As aforementioned, viscosity is often attributed as a strong influence on DE. Generally, the higher the viscosity of the oil, the less effectively it is dispersed when chemical dispersants are applied. The data collected for this study supports this general trend. Kinematic viscosity was calculated against DE for each oil-temperature combination. Relationships were evaluated by comparing correlation coefficients of linear trend lines. The correlation coefficient was interpreted using Table 9.

Table 9. Interpretation of Correlation Coefficients [21].

Size of Correlation	Interpretation
0.90 to 1.00	Very high correlation
0.70 to .90	High correlation
0.50 to .70	Moderate correlation
0.30 to .50	Low correlation
0.00 to .30	Negligible correlation

Figure 20 and Figure 21 focus on the relationship between viscosity and DE at 20ºC and 5ºC, respectively. At both temperatures, Finasol generally has a higher DE, and the relationship between viscosity and DE is slightly stronger. There is a moderate correlation between viscosity and DE for Corexit 9500A and a low correlation between viscosity and DE for Finasol at 20ºC. Since neither dispersant has a high correlation at 20ºC, it can be assumed that there are other variables affecting DE. Both dispersants have a high correlation between kinematic viscosity and DE at 5ºC. The division between low/medium crude oils and heavy oils can be identified by the two distinct groupings of data points in Figure 20. This could be responsible for the high correlation.

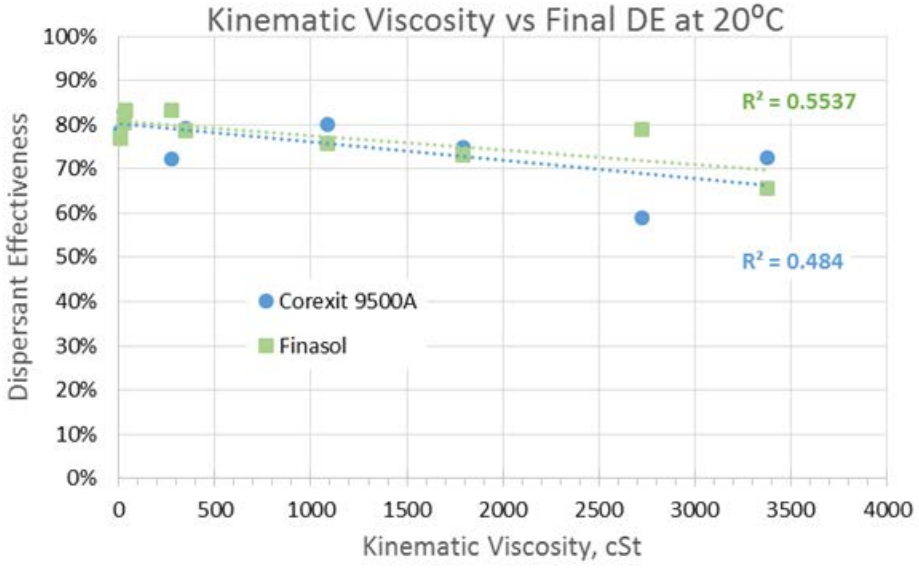

Figure 20. Comparison of the effectiveness of Corexit 9500A and Finasol to the viscosity of crude oil at 20^{0}C.

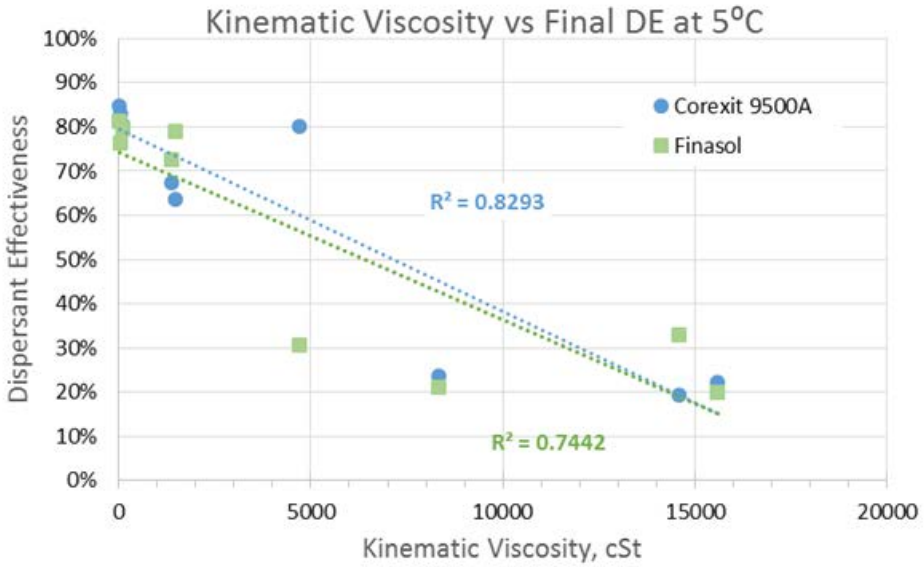

Figure 21. Comparison of the effectiveness of Corexit 9500A and Finasol to the viscosity of crude oil at 5°C.

Figure 22 and Figure 23 are a rearrangement of the same data above to emphasize the temperature effect for each dispersant. The correlation between viscosity and DE for both Corexit 9500A and Finasol at 5ºC is significantly stronger than at 20ºC.

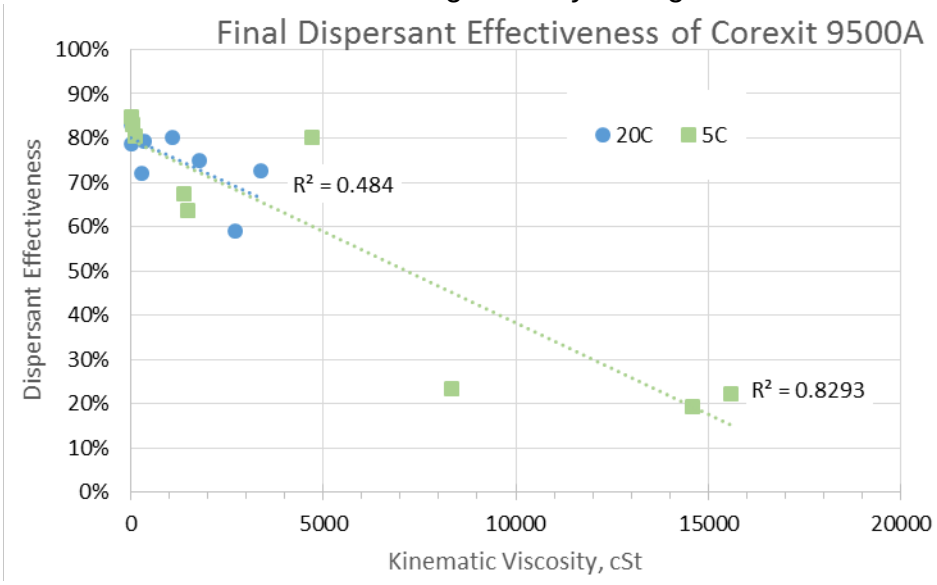

Figure 22. Comparison of the effectiveness of Corexit 9500A at 5ºC and 20ºC.

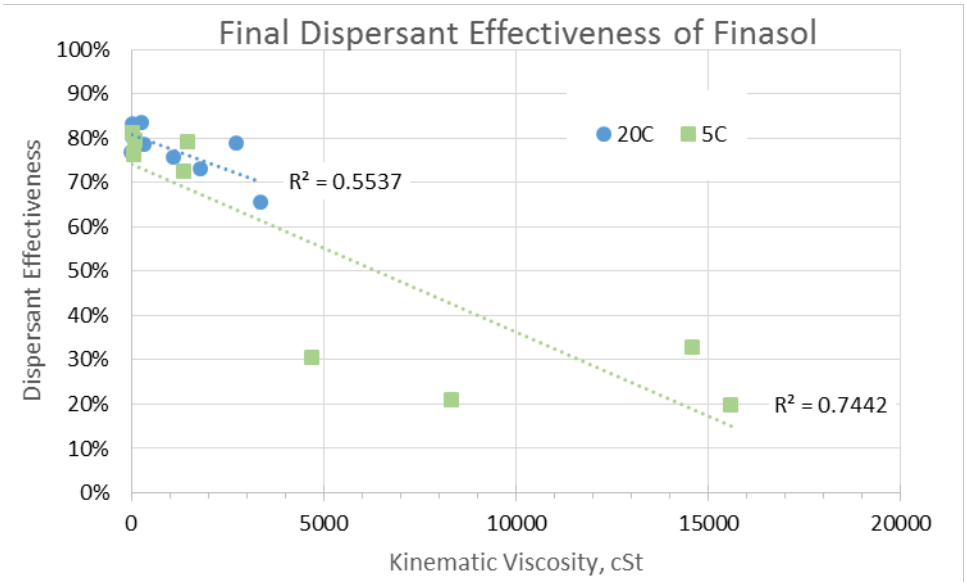

Figure 23. Comparison of the effectiveness of Finasol at 5ºC and 20ºC.

Figure 24 through Figure 27 further reinforce that although there is a general correlation between DE and viscosity, there are secondary factors that influence DE. Figure 24 and Figure 25 show the DE of crude oils dispersed by Corexit 9500A in ascending order of kinetic viscosity, with low viscosities on the left and high viscosities on the right. It is interesting to note that the order of the oils are almost identical at both temperatures. DE fluctuates up and down mirrored at both temperatures with a general trend downwards as viscosity increases.

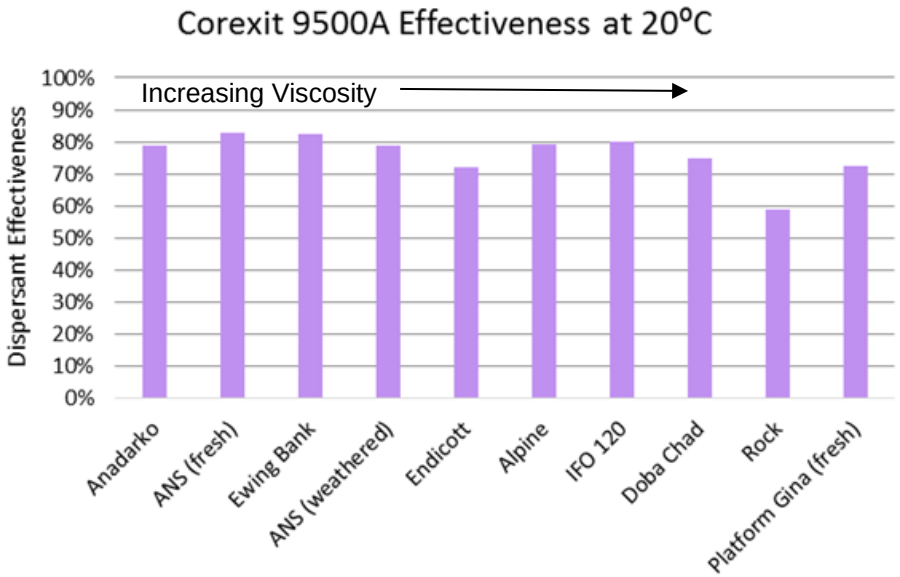

Figure 24. The effectiveness of Corexit 9500A at 20ºC as oil viscosity increases.

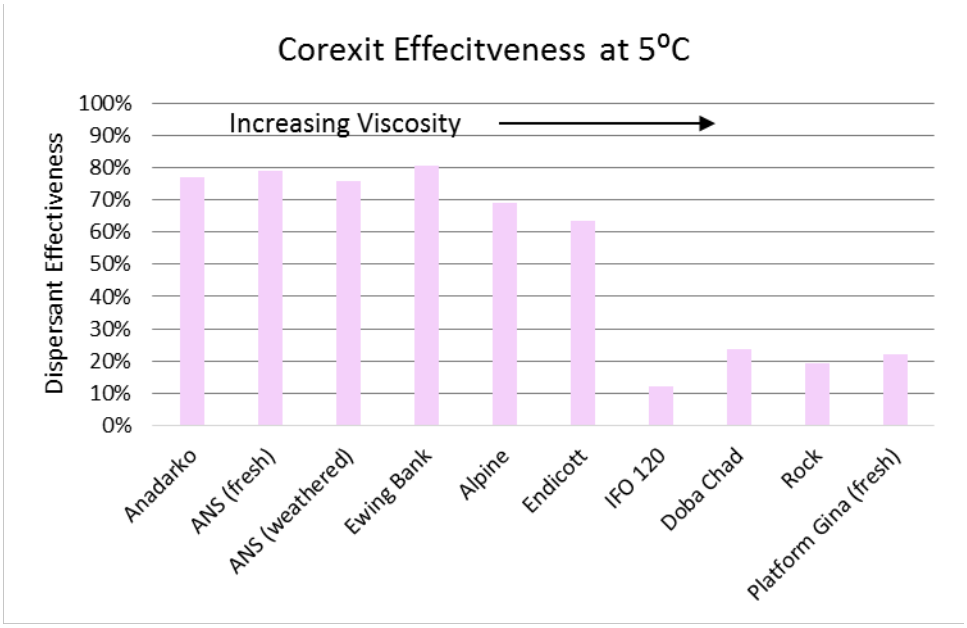

Figure 25. The effectiveness of Corexit 9500A at 5°C as oil viscosity increases.

Figure 26 and Figure 27 show the DE of crude oils treated with Finasol in ascending order of kinetic viscosity, with low viscosities on the left and high viscosities on the right. Finasol at 20°C follows the same fluctuating trend downwards that was seen with Corexit 9500A at 20°C. The dramatic shift in dispersant effectiveness between Endicott and IFO120 at 5°C is to be expected, as the change in viscosity is about 3000 cSt.

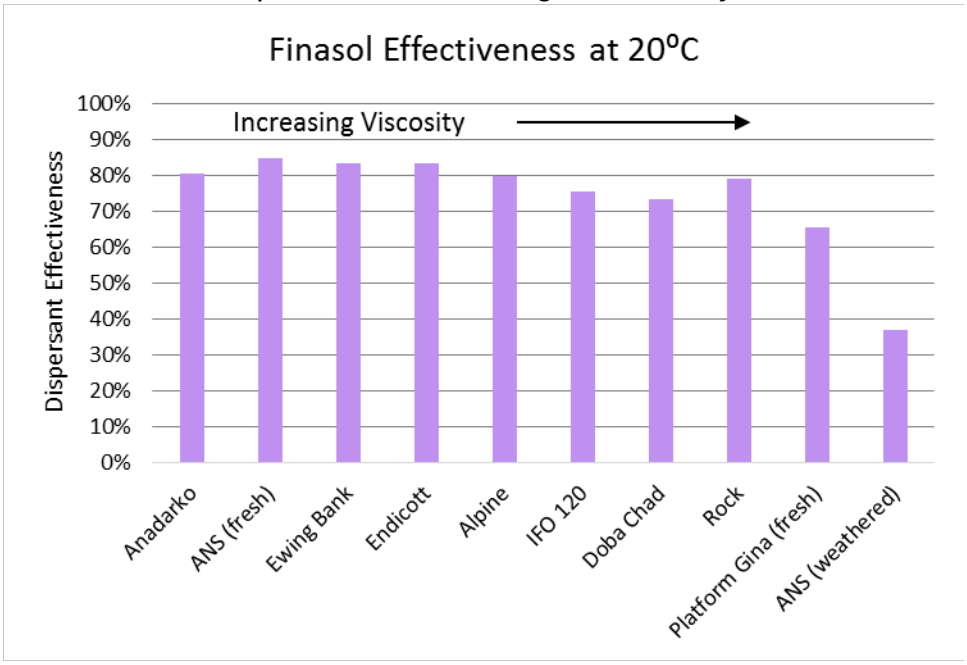

Figure 26. The effectiveness of Finasol at 20°C as oil viscosity increases.

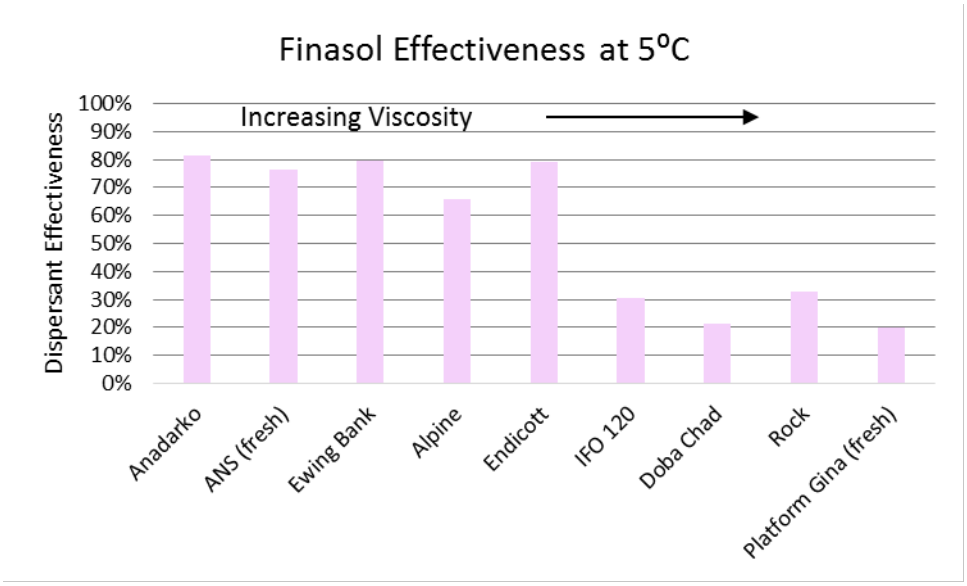

Figure 27. The effectiveness of Finasol at 5ºC as oil viscosity increases.

3.8. HYDROCARBON GROUPS — SARA

As aforementioned, the components of oil are often broadly grouped into four categories: saturates, aromatics, resins, and asphaltenes (SARA). Since increasing viscosity and decreasing DE were not consistently highly correlated, perhaps there may be a correlation between DE and one of the hydrocarbon groups; however, the data collected in this study does not reflect that assumption. Figure 28 through Figure 31 depict the relationship between each hydrocarbon group and the DE of Corexit 9500A at both 20ºC and 5ºC. For Corexit 9500A, there was a negligible correlation between DE and saturates, aromatics, and resins. There was a low correlation between asphaltenes and DE, with the correlation coefficient higher at 20ºC. For Finasol, the correlation between the hydrocarbon groups was more temperature-dependent. There was negligible correlation between DE and all four hydrocarbon groups at 20ºC for Finasol. At 5ºC, however, there was a high correlation between aromatics and resins and DE, and a moderate correlation between asphaltenes and DE.

3.8.1. DE as a function of SARA concentration for Corexit 9500A

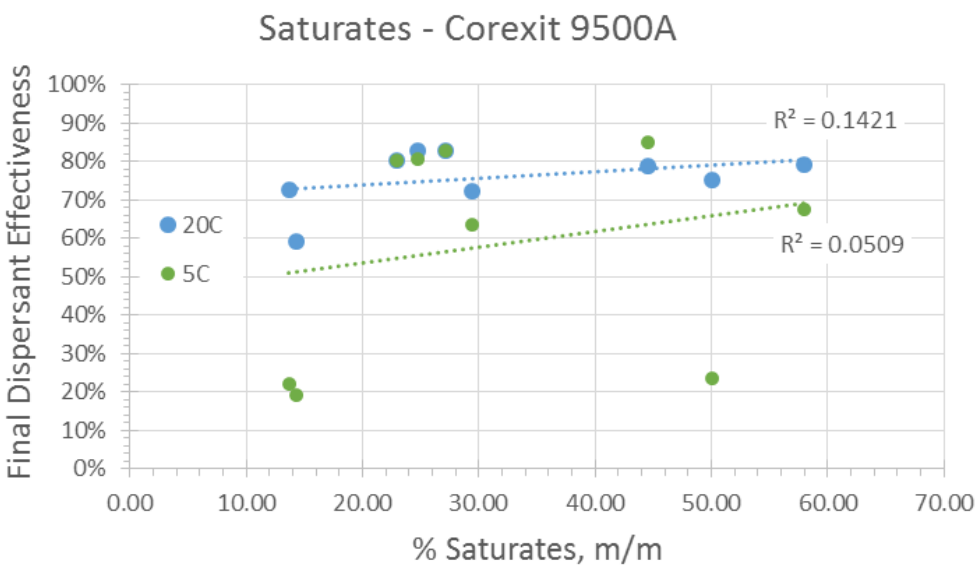

Figure 28. Correlation between saturate content and the effectiveness of Corexit 9500A at 5^{0}C and 20^{0}C.

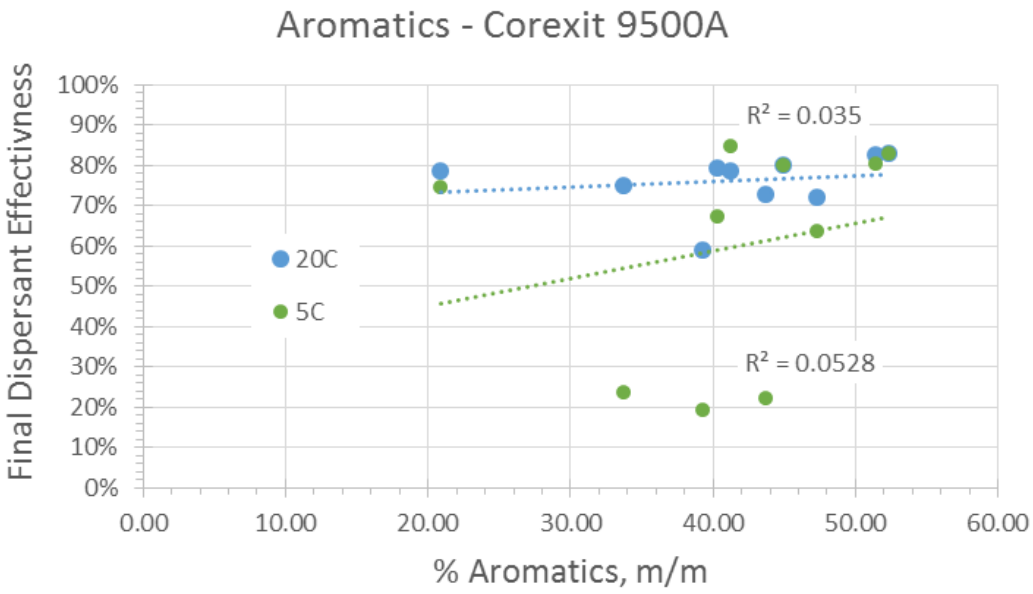

Figure 29. Correlation between aromatic content and the effectiveness of Corexit 9500A at 5^{0}C and 20^{0}C.

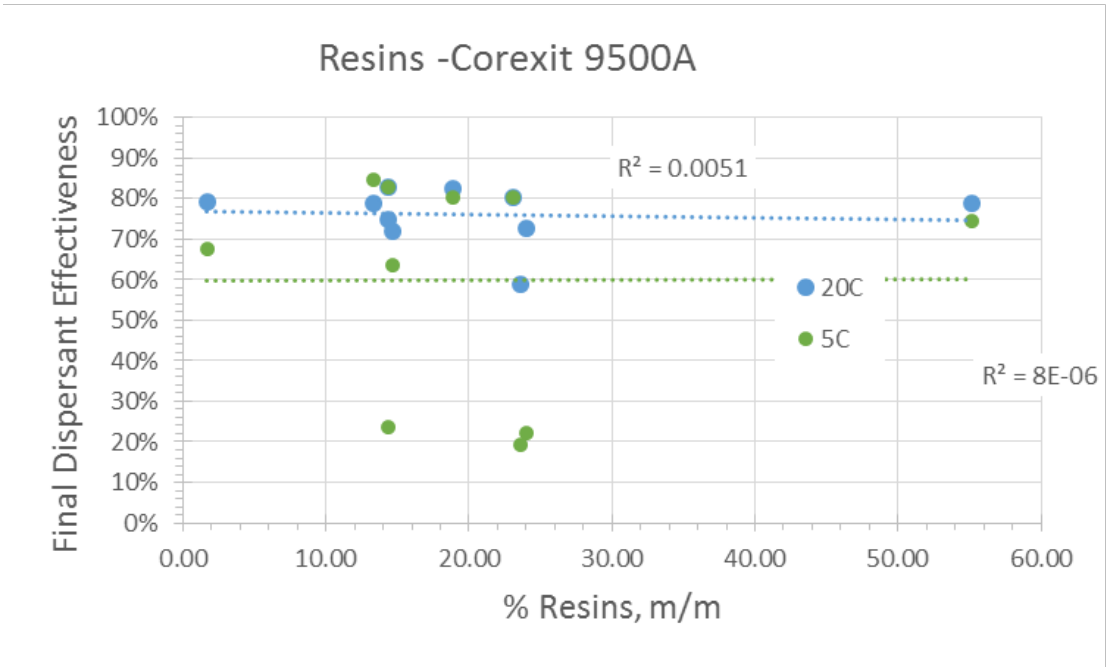

Figure 30. Correlation between resin content and the effectiveness of Corexit 9500A at 5^0C and 20^0C.

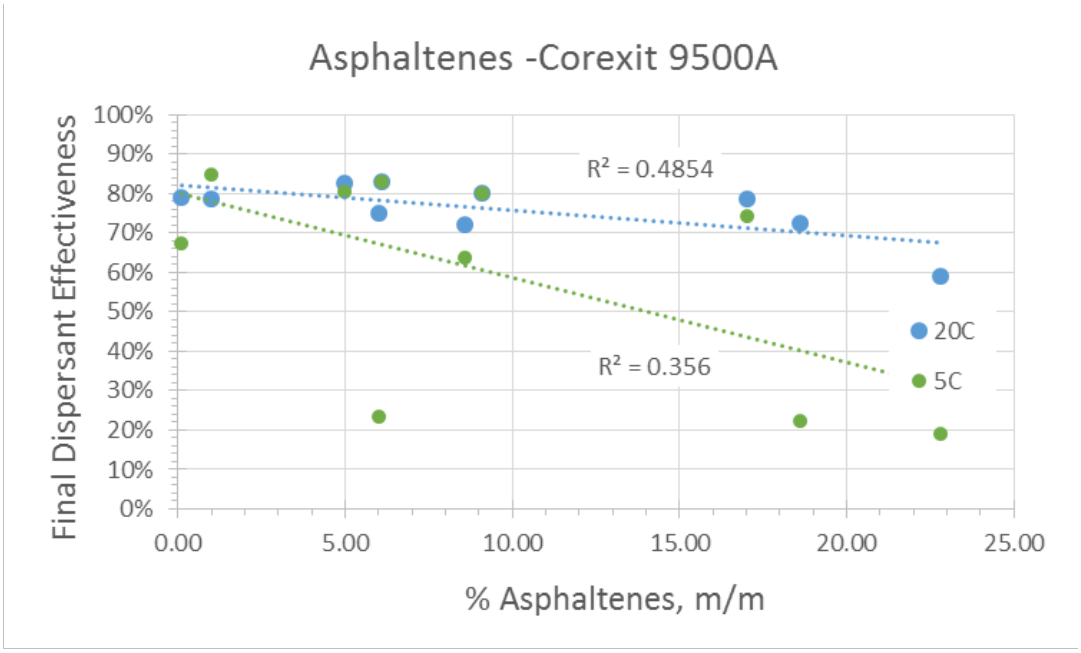

Figure 31. Correlation between asphaltene content and the effectiveness of Corexit 9500A at 5^0C and 20^0C.

3.8.2. DE as a function of SARA Concentration for Finasol

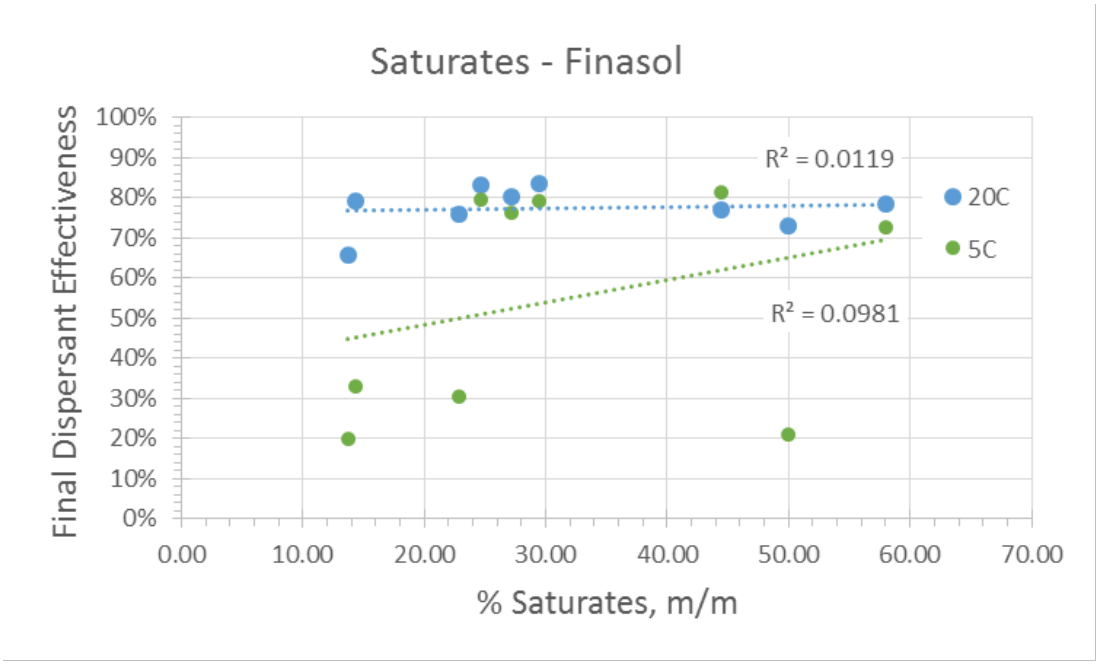

Figure 32. Correlation between saturate content and the effectiveness of Finasol at 5^{0}C and 20^{0}C.

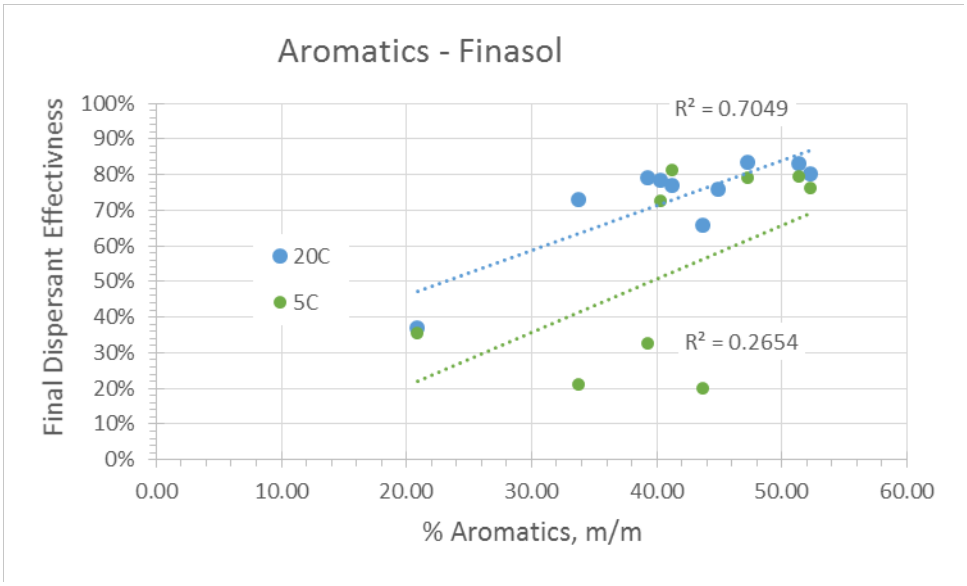

Figure 33. Correlation between aromatic content and the effectiveness of Finasol at 5^{0}C and 20^{0}C.

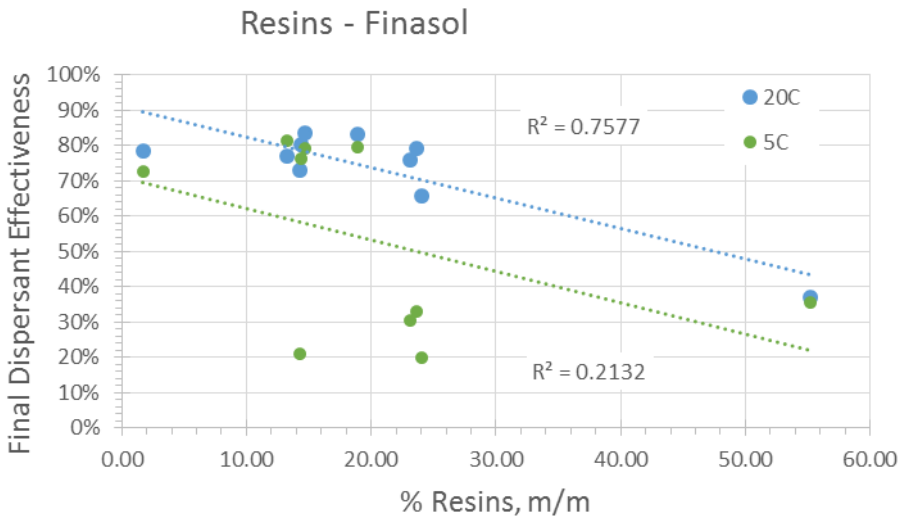

Figure 34. Correlation between resin content and the effectiveness of Finasol at 5^{0}C and 20^{0}C.

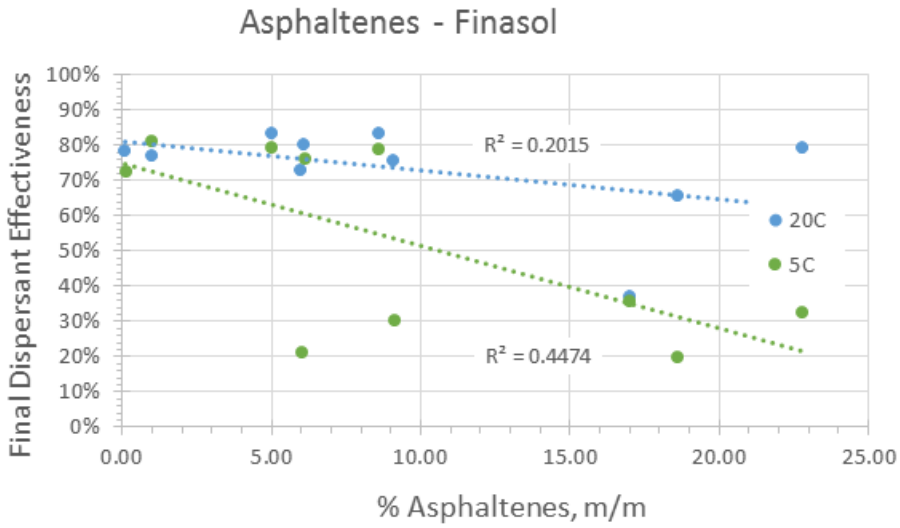

Figure 35. Correlation between asphaltene content and the effectiveness of Finasol at 5^{0}C and 20^{0}C.

4. LASER IN-SITU SCATTERING TRANSMISSOMETRY (LISST)

When performing DE measurements at Ohmsett or in the field, the oil spill response community traditionally relies on measuring the amount of oil with droplets sizes below 70 µm as a measure of the DE; oil droplets below 70 µm diameter tend to stay dispersed in the water column [4]. While useful, this measure of DE is fundamentally different than the BFT method, which measures the total amount of oil dispersed in the water instead. To provide a direct comparison between the DE measured with the BFT and DE measured with the LISST, we used samples from the same baffled flask for each replicate for both measurements. Since oil is a dynamic changing material, we followed a systematic procedure to minimize the inherent variability in these samples.

4.1. LISST Measurement Procedure

The procedure is described below.

1. Clean the LISST chamber with rubbing alcohol before each test.
2. Keep the temperature of deionized water at the same temperature as the BFT sample using the temperature controlled shaker table.
3. After 10 minutes of settling following mixing, immediately remove baffled flask from the shaker table.
4. Discard a 2-mL sample through the stopcock from the bottom of flask.
5. Using a 50-mL graduated cylinder, measure a 30-mL sample through the stopcock from the bottom of the flask and use for BFT liquid-liquid extraction.
6. Using a 10-mL graduated cylinder, measure a 6-mL sample through the stopcock from the bottom of the flask.
7. Add 50 mL deionized water into the LISST chamber, then measure the temperature. Add the 6-mL sample from the baffled flask into the chamber, then add another 50 mL deionized water to provide mixing energy without inserting any foreign objects into the solution to stir (to prevent sample contamination).
8. Start collecting LISST data for 15 minutes at one-second intervals as shown in Figure 36.

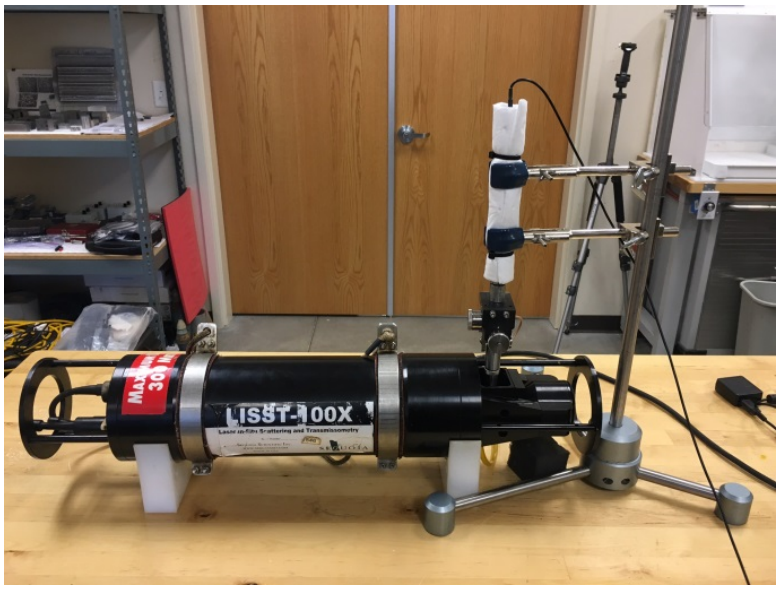

Figure 36. Experimental setup for the LISST and acoustic measurements. The acoustic measurements will be described separately.

9. Measure the temperature of diluted solution after LISST testing.
10. Drain the oil solution into the waste container after collecting data.
11. Clean the lens of LISST and the chamber with rubbing alcohol after the test is complete.

4.2. LISST DE CALCULATION

The LISST instrument measures the particle size distribution by transmitting light through the solution of oil droplets in water and collecting the scattered light on a series of concentric rings. The smallest ring collects the light scattered from the larger droplets and the largest ring collects the light scattered from the smallest droplets. The size of the particle size bins is dictated by the width of the ring. A screen shot of the output from the LISST is shown in Figure 37. The left portion shows the droplet size distribution and the right shows the cumulative concentration represented as a percentage of droplets as a function of droplet size.

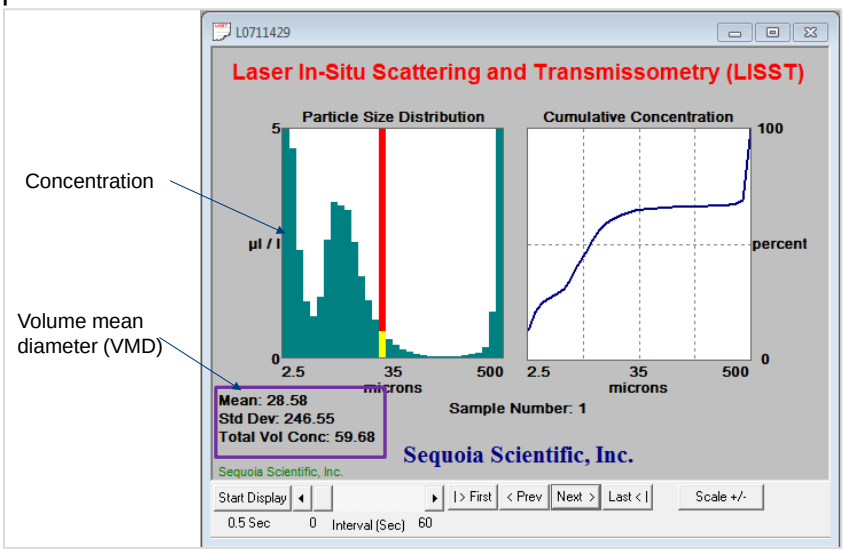

Figure 37. Screen shot from the LISST measurement software

The resultant droplet size distribution for four replicates of ANS with Corexit at 20°C at a DOR of 1:25 is shown in Figure 38 along with the average of the four replicates in the bottom figure. To determine the dispersant effectiveness from these data, one needs to calculate the amount of oil with droplets sizes below 70 µm. Since the concentric detector rings of the LISST do not split on either side of 70 µm, we chose to calculate the dispersant effectiveness as the percentage of oil with droplet size below 74.5 µm.

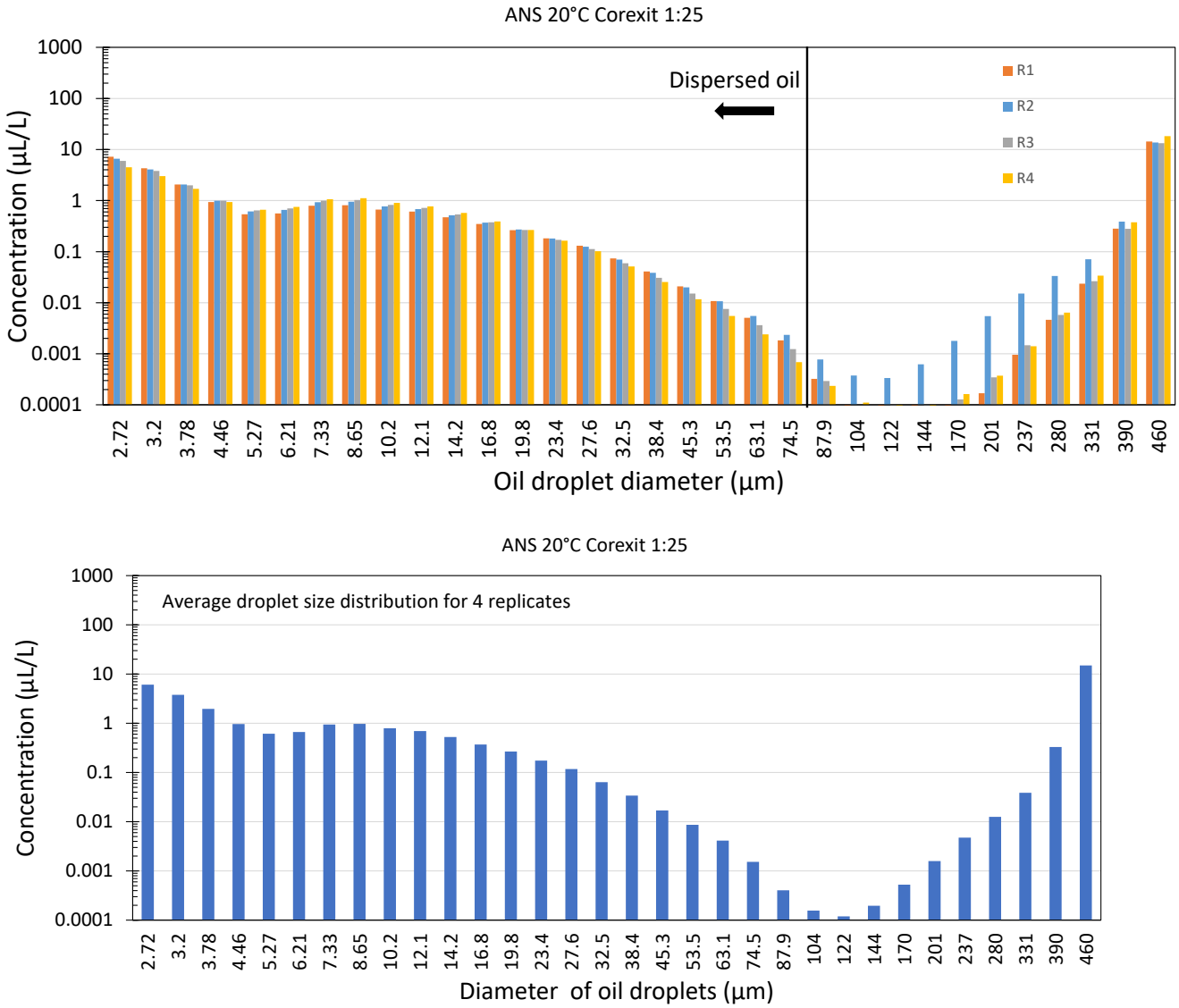

Figure 38. Droplet size distribution from the LISST for ANS at a DOR of 1:25 for Corexit 9500.

To visually see the percentage of oil droplets that have sizes below 70 mm, Figure 39 shows the cumulative concentration as a function of droplet size. In this case, the dispersant effectiveness can be read from the graph by following the intersection of the vertical and horizontal lines to the percentage axis to read the value of ~56% for the dispersant effectiveness. Using this method to determine dispersant effectiveness, we calculated the DE in over one-minute intervals for the entire 15-minute duration of the experiment. We chose to measure the DE over multiple minutes to determine if any agglomeration of breakup of the droplets occurred. The data for this set of experiments shown in Figure 40 do not show and indication of agglomeration of break-up. Replicate 4 shows a lower dispersant effectiveness between three and 10 minutes but agrees with the other replicates otherwise. This type of behavior was common, where one replicate deviated from the others. The average and standard deviation are shown for the four

replicates. The resultant dispersant effectiveness was calculated as the average of all replicates over the entire 15-minute measurements time.

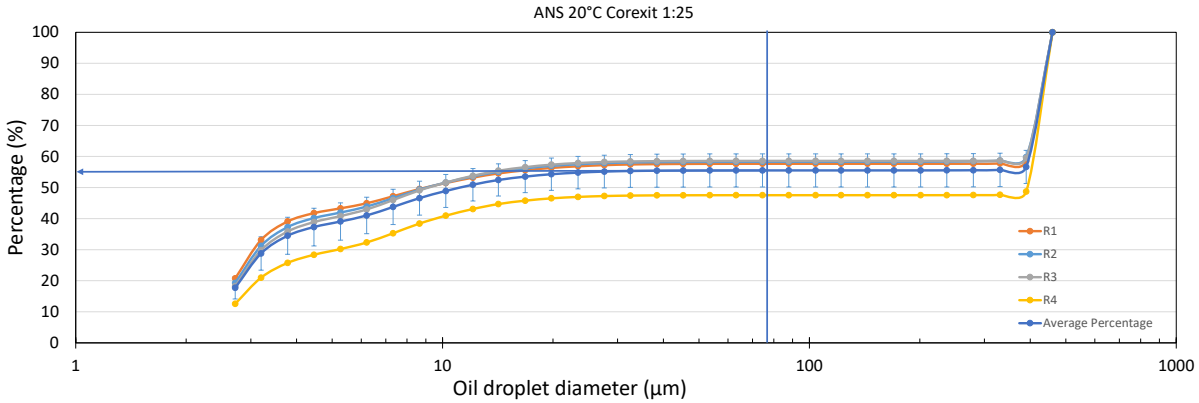

Figure 39. The cumulative concentration of ANS for four replicates along with the average of all replicates as a function of droplet size.

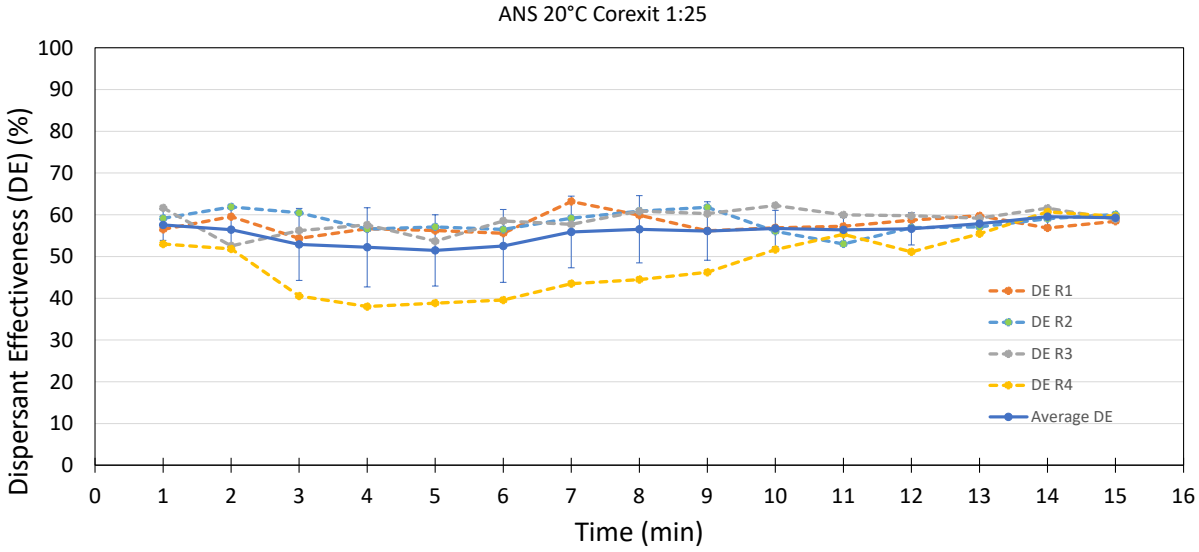

Figure 40. The resultant DE from the LISST over the 15-minute measurement period.

4.3. COMPARISON BETWEEN LISST AND BFT

The dispersant effectiveness calculated from the LISST is consistently lower than the DE calculated from the BFT, as shown in Figure 42. The differences between the BFT and LISST are even larger at 5°C. Some reasons why the two measurements of DE are different can be related to fact that they are measuring two distinctly different properties of the dispersed oil. In the BFT, the DE is determined based on the amount of oil that is in the water-oil mixture, while in the LISST, measurement of the DE is determined as the percentage of oil with droplet sizes below 74.5 µm. Figure 38 shows there are a significant number of droplets in the water-oil mixture with sizes above 74.5 µm. In the BFT, all of this oil is measured (even larger droplets) as dispersed, which may be a cause for the disagreement in DE between the two methods. Another contribution may come from

mixing the sample from the baffled flask in the LISST chamber during dilution. That dilution process may strip the dispersant from the oil droplets further allowing the oil droplets to coalesce; though there is evidence that bonding of dispersant particles at the oil water interface is irreversible [4] and we did not see significant changes in the DE over a 15-minute time span. At this time, it is unclear why the difference is so large, but it is clear that additional study is needed in the lab and during Ohmsett testing to determine which method is most representative of the DE and what is causing the discrepancy.

Table 10. DE for both the BFT and LISST measurements for the oils at 20°C.

Oil	Kinematic Viscosity, cSt	BFT DE LCL_{95DE}	LISST DE	Crude Category by kinematic viscosity
ANS (fresh)	25	83.86%	55.9%	medium
Alpine	317	80.44%	47.9%	heavy
Doba Chad	1657	75.04%	52.5%	heavy
Platform Gina (fresh)	3244	57.79%	40.9%	heavy

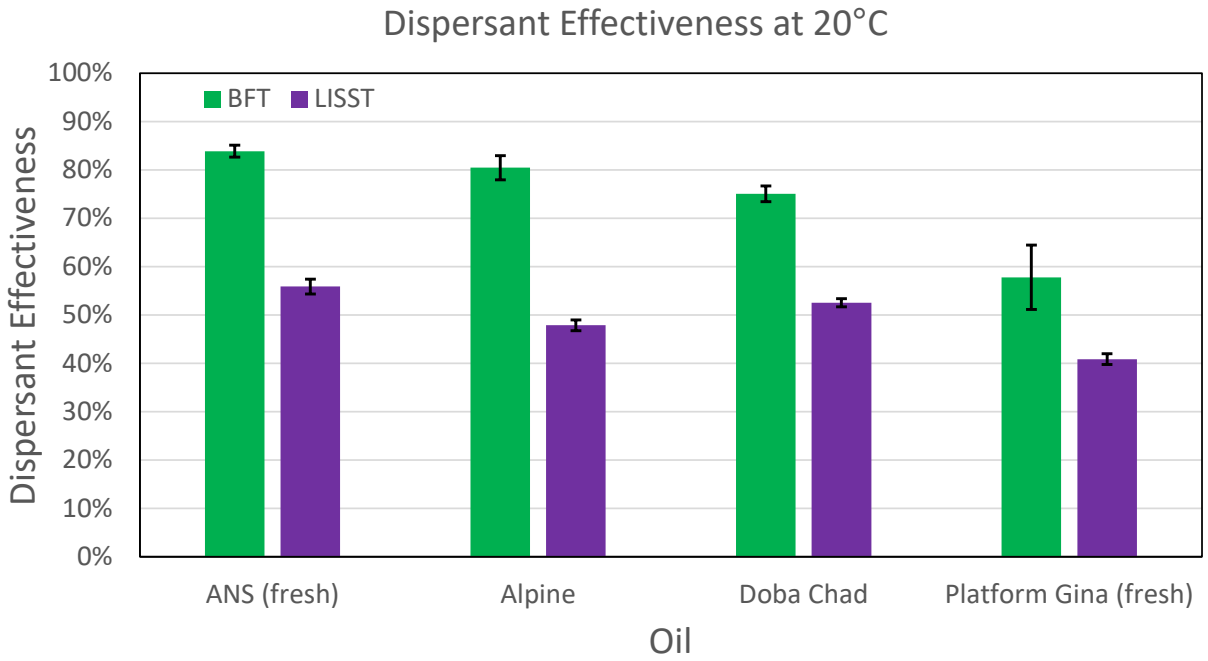

Figure 41. The dispersant effectiveness at 20°C using the BFT and LISST measurements.

Table 11. DE for both the BFT and LISST measurements for the oils at 5°C.

Oil	Kinematic Viscosity, cSt	BFT DE LCL_{95DE}	LISST DE	Crude Category by kinematic viscosity
ANS (fresh)	49	79.16%	3.4%	medium
Alpine	1368	69.18%	2.6%	heavy
Doba Chad	8321	23.82%	1.7%	heavy
Platform Gina (fresh)	15592	22.23%	0.9%	heavy

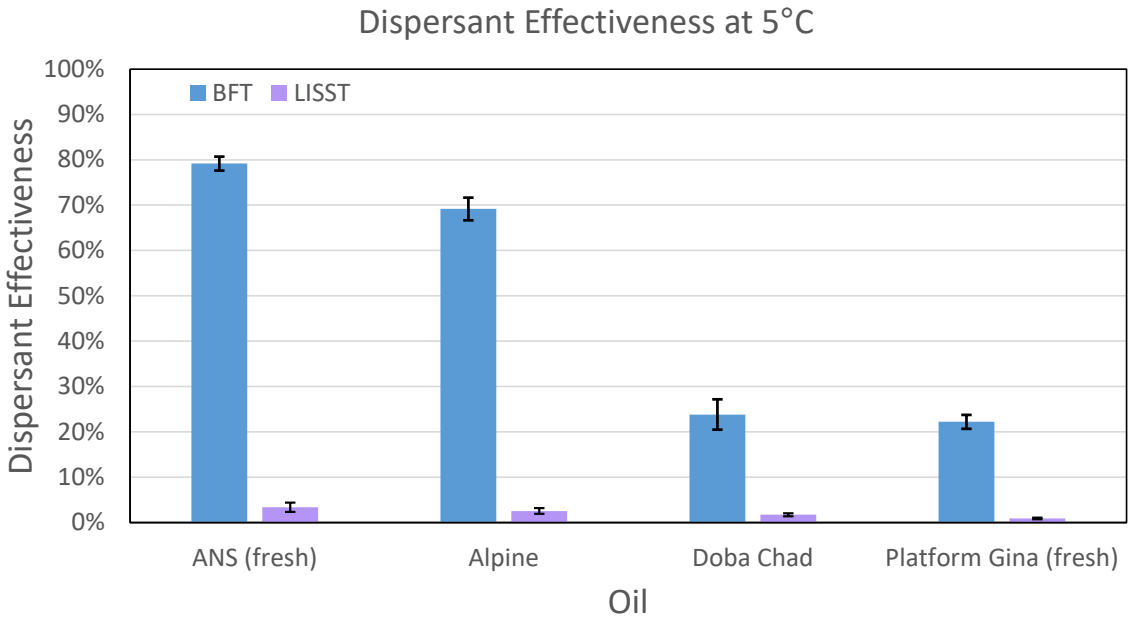

Figure 42. The dispersant effectiveness at 5°C using the BFT and LISST measurements.

5. ACOUSTIC BACKSCATTERING MEASUREMENT OF DISPERSED OILS

As part of this work, measurements on the dispersed oils using acoustic scattering measurements were previously developed by the team. The purpose of these measurements was to develop robust measurements of DE and droplet size distribution that would overcome the measurement issues when the LISST optics become fouled with oil or when ceases to collect data at high concentrations. The acoustic measurements were performed simultaneously with the LISST measurements to provide the opportunity to benchmark the acoustic measurements. A theoretical model for the backscattering was also explored to help move towards the goal of determining a droplet size distribution.

5.1. THEORETICAL BACKSCATTER MODEL

Acoustic scattering interactions with oil droplets may be characterized by a scattering cross section. When an acoustic transducer is placed far from a scattering materials, a fraction of the total scattered power is received by the transducer. The relevant measure is the backscatter coefficient, which is defined as the differential scattering cross-section

per unit volume per unit solid angle at an angle of 180°. For a continuum scattering model, the backscatter coefficient $\eta(k)$ may be expressed as Equation 9 [16]:

$$\eta(k) = \frac{k^4 \langle \gamma^2 \rangle}{16\pi^2} \iiint d\left(\Delta\vec{r}\right) b\left(\Delta\vec{r}\right) e^{-i\vec{k}\cdot\Delta\vec{r}} \tag{9}$$

where $k = \omega / c$ is the wave number, ω is the angular frequency, and c is the speed of sound in the medium. $\langle \gamma^2 \rangle$ is the mean square fluctuation of the parameter γ, which is related to the scattering strength of the random medium, and $b\left(\Delta\vec{r}\right)$is the normalized spatial autocorrelation function for the medium. We will assume that the medium is isotropic so that we need consider only the magnitude of $\Delta\vec{r}$ in the spatial autocorrelation function thus we can replace $b\left(\Delta\vec{r}\right)$ with $b(\Delta r)$.

In general, the spatial autocorrelation function $b(\Delta r)$ describes the similarity of the mass density and compressibility at two positions in the scattering volume separated by the distance Δr. Figure 43 shows a schematic of a two-component scattering medium. We consider Δr the length of a line placed arbitrarily in the scattering medium. We define P_{ab} as the probability that one end of the line is in environment *a*, the other end will be in environment *b*. Thus, four probabilities—P_{00}, P_{01}, P_{10}, P_{11}—exist, where the subscript "0" stands for background material and "1" for a scatterer. For the case of a distribution of scatterers with random sizes and shapes, the scattering can be approximately characterized by an exponential autocorrelation function.

The spatial autocorrelation function for a two-component medium was proposed by Yagi [17]. In Yagi's model, the spatial autocorrelation function for a two-component medium is represented by the sum of two exponential terms.

$$b_y(\Delta r) \approx 0.40e^{-\frac{\Delta r}{0.53(1-H)r_y}} + 0.60e^{-\left(\frac{\Delta r}{0.92(1-H)r_y}\right)^2} \tag{10}$$

Where r_y is the characteristic radius of scatterers and H is the scatterer volume fraction in the medium.

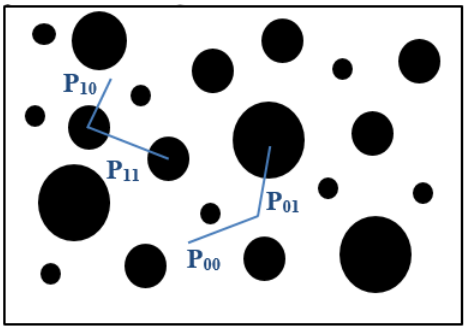

Figure 43. For a two-component scattering medium, we consider Δr the length of a rod thrown arbitrarily into the medium. We define P_{ab} as the probability that with one end of the rod in environment *a*, the other end will be in environment *b*. Thus, four probabilities—P_{00}, P_{01}, P_{10}, P_{11}—exist, where the subscript 0 stands for background material and 1 for a scatter [18].

The backscattering coefficient is determined by taking the Fourier transform of the spatial autocorrelation function $b_y(\Delta r)$. For Yagi's model, the backscatter coefficient is given by [17]:

$$\eta_y(k,H) \approx \frac{k^4 r_y^3}{12\pi}\left(\frac{\Delta\kappa}{\kappa}-\frac{\Delta\rho}{\rho}\right)^2 H(1-H)^4 \left\{\frac{0.37}{\left[1+1.1k^2 r_y^2 (1-H)^2\right]^2}+0.63e^{-0.85k^2 r_y^2 (1-H)^2}\right\} \quad (11)$$

where $\Delta\kappa = \kappa_1 - \kappa_0$, $\kappa_i = \frac{1}{\rho_i c_i^2}$ is defined as the compressibility. In $\Delta\rho = \rho_1 - \rho_0$, 0 and 1 refer to the background material and the scatters. *H* represents the scatter volume fraction in the medium, it is related to the concentration of oil.

Figure 44 shows the theoretical prediction of the backscatter coefficient as a function of frequency while varying the characteristic radius of scatterers r_y and the scatter volume fraction *H* while fixing *H*=0.0005 µL/L and r_y=10 µm, respectively. It can be seen that the backscatter coefficient increases as the characteristic radius r_y and the scatter volume fraction *H* increase.

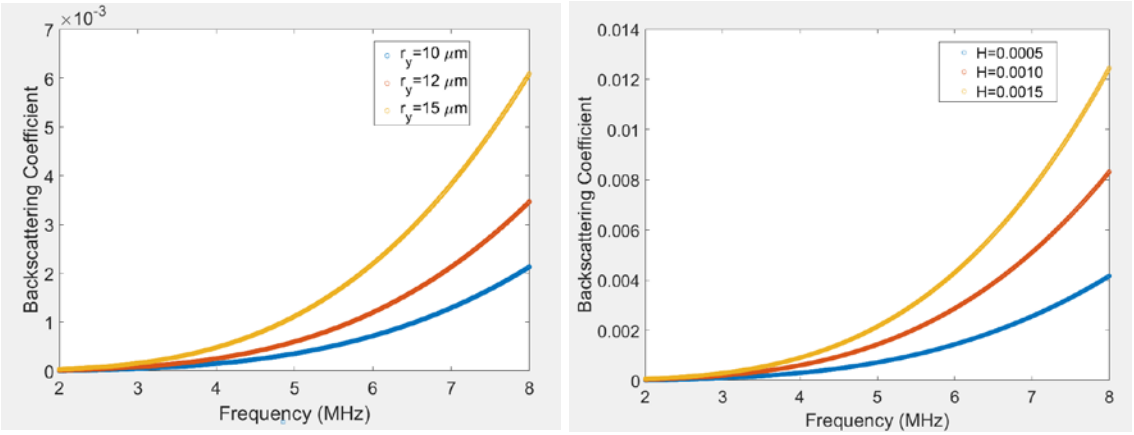

(a) (fixed *H*=0.0005 µL/L) (b) fixed r_y=10 µm

Figure 44. Simulated backscatter coefficients as a function of frequency with varying r_y (a) and *H* (b), respectively.

The theory described assumes a Gaussian particle size distribution; however, the particle size distribution measured by the LISST showed a bimodal distribution with many particles below ~100 µm and often more above ~100 µm. Thus, a direct comparison between the theory and the experimental data is not a valid approach at this time. To further these acoustic measurements to provide a droplet size distribution, a theoretical formulation that allows for an arbitrary particle size distribution will be needed.

5.2. Acoustic Backscatter Experiment

Figure 45 shows the schematic of the ultrasonic backscatter measurement in the dispersed oil solution. The blue circles indicate the dispersed oil droplets. The transducer emits the ultrasonic pulses into the sample and receives the scattered signals. Figure 46

shows the experimental setup for the backscatter measurement. The transducer with a central frequency of 10 MHz was immersed into the 60-mL dispersed oil solution, which was collected from the stopcock from the bottom of baffled flask. The right image of Figure 46 shows a backscattered signal from dispersed oil droplets.

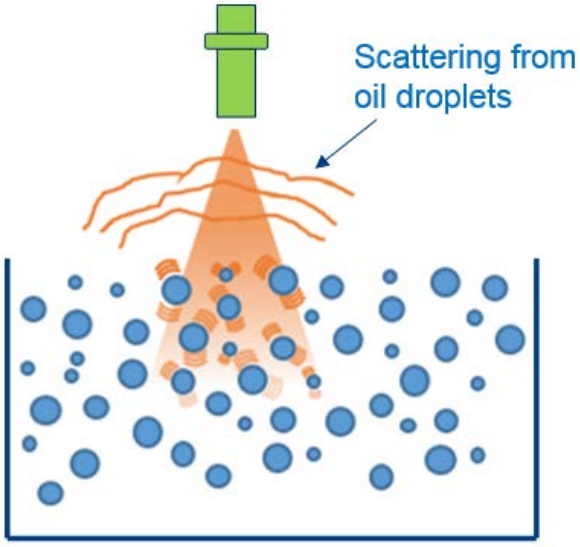

Figure 45. The schematic of the ultrasonic backscatter measurement in the dispersed oil solution.

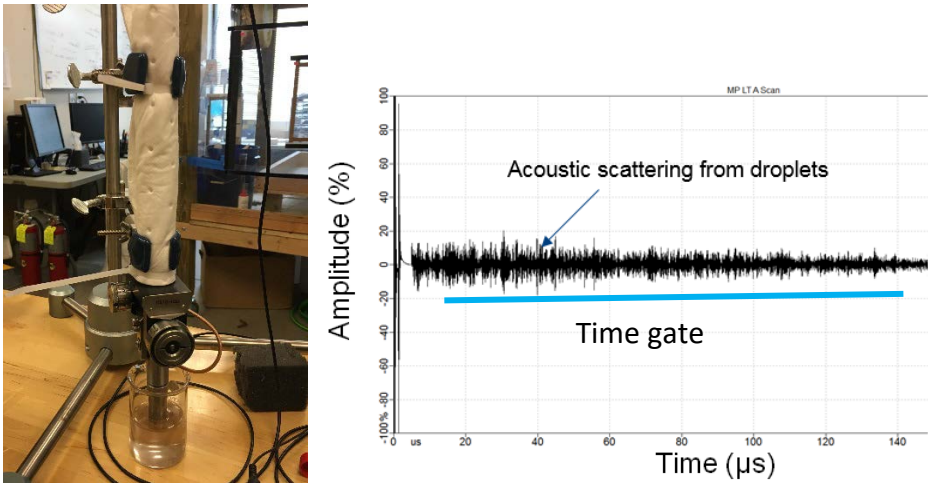

Figure 46. The experimental setup for the backscatter measurement using a transducer with a central frequency of 10 MHz (a), a backscattered signal reflected from oil droplets.

A time gate was set to choose the time range to calculate the Fourier transform of the backscattered signals. Figure 47(a) shows the fast Fourier transform (FFT) of the backscattered signal. A reference signal was also collected from the reflection from fused silica block and was used to remove the frequency response and effects of the electronics from the backscattering signal. Figure 47 (b) shows the FFT of the reference signal. The experimental backscatter coefficient is calculated as the ratio of the Fourier amplitude of backscattered signals to the Fourier amplitude of the reference signal.

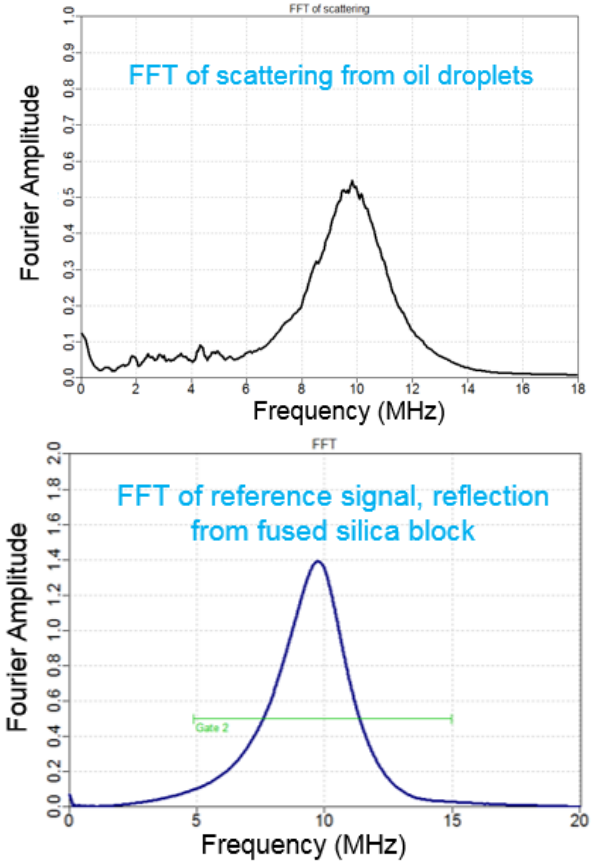

Figure 47. The FFT of the collected backscattered signals (top); the reference signal reflected from a silica block (bottom).

Figure 48 shows the experimental backscatter coefficient as a function of frequency for the oils and 5°C and 20°C. The legend has the oils listed in ascending viscosity. Two features of the backscattering that are indicative of the properties of the material are the amplitude of the backscattering and the frequency response. Figure 49 demonstrates the amplitudes of the backscatter coefficients corresponding to the central frequency (10 MHz) of the transducer verse the DE as measured by the LISST for four replicates for four oils at 5°C for Corexit 9500. The round circles represent the replicates for each oil. The triangles indicate the average over four replicates for each oil. Corresponding graph for the oils at 20°C is shown in Figure 50. The horizontal and vertical error bars indicate the standard deviation of the dispersant effectiveness and the backscatter amplitudes over four replicates for each oil. It can be seen that the amplitude of the backscatter coefficient at 10 MHz increases approximately linearly as the DE increases with a stronger linear relationship at 20°C.

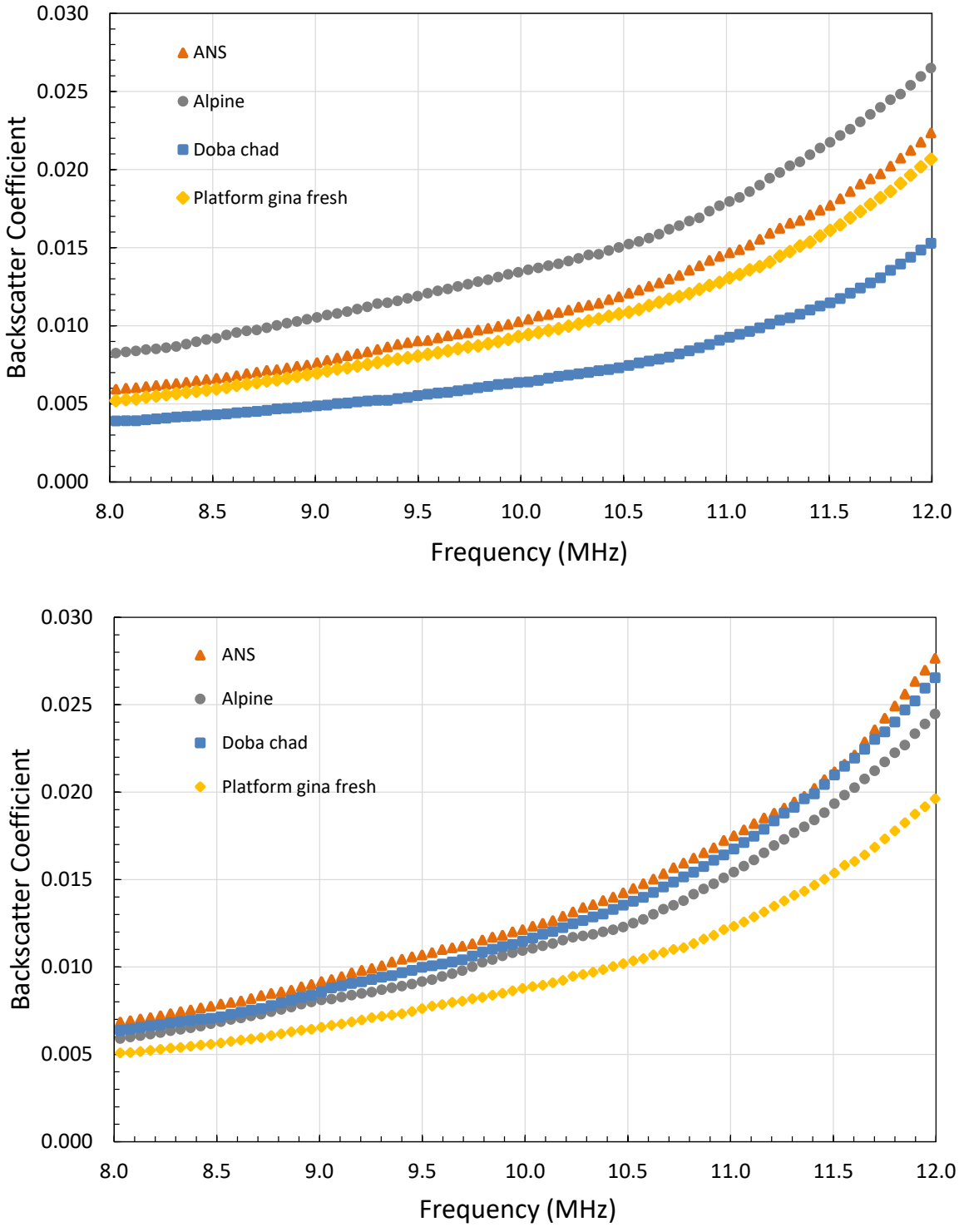

Figure 48. The backscatter coefficients averaged over four replicates for four oil at 5°C (top) and 20°C (bottom).

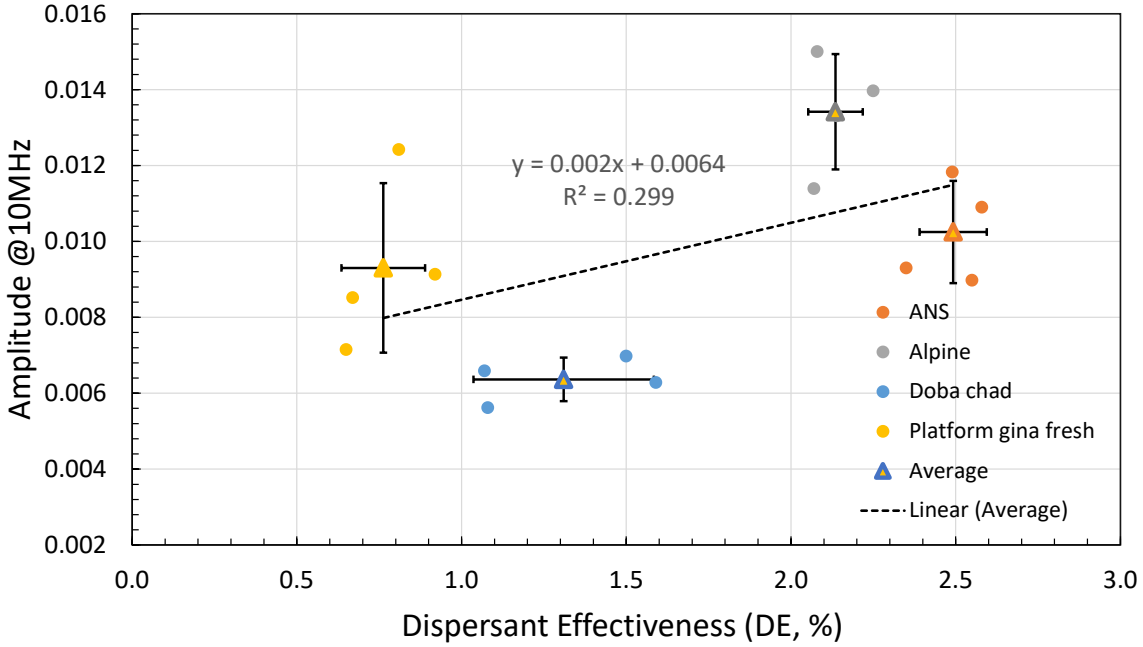

Figure 49. The amplitude of the backscatter coefficient at 10 MHz versus the DE for four replicates for four oils at 5°C.

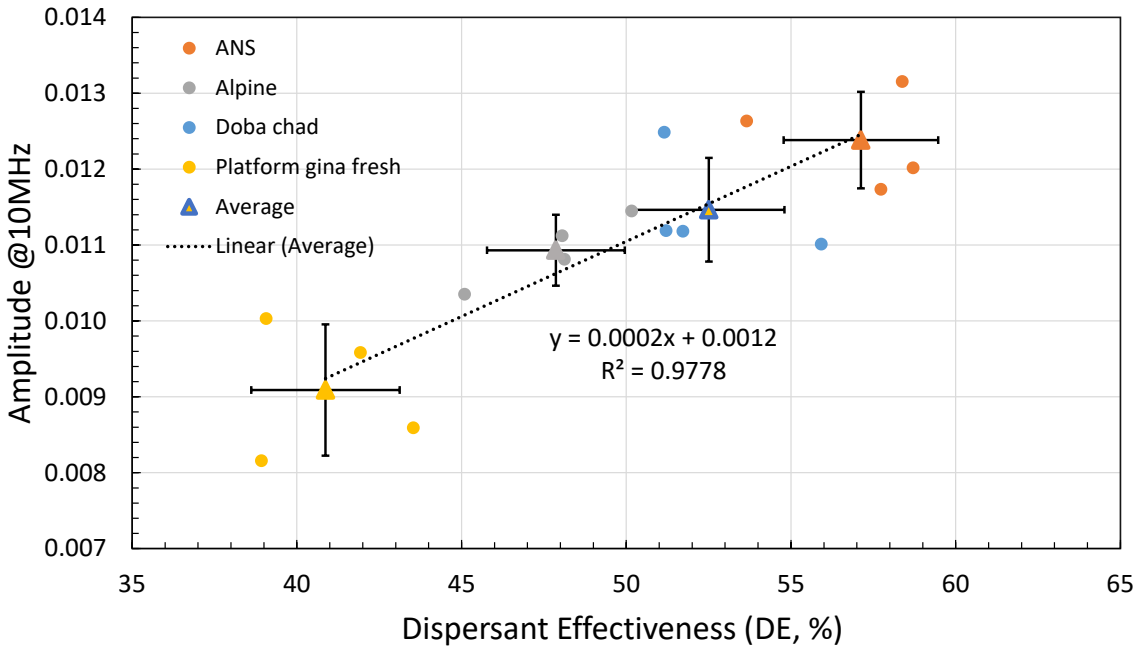

Figure 50. The amplitude of the backscatter coefficient at 10MHz versus the DE for four replicates for four oils at 20°C.

Figure 51 shows the amplitudes of the backscatter coefficients for crude oils of the ANS and Doba chad versus the d_{50}, which defines the diameters of scatterers corresponding to 50% percentage volume fraction in the particle size distribution (PSD). The value of the d_{50} can be determined from the cumulative percentage of oil droplets

measured from the LISST; however, for the Alpine and Platform Gina fresh, the total percentage of dispersed oil droplets with the diameter less than 400 μm is lower than 50%. Therefore, the d_{50} cannot be determined from the cumulative percentage of oil droplets measured from the LISST for the Alpine and Platform Gina fresh. To investigate the dependence of amplitudes on oil droplets sizes, we choose the d_{30} for four replicates of each oil. Figure 52 shows the amplitudes of the backscatter coefficients versus the d_{30}, which defines the diameters of scatterers corresponding to 30% percentage volume fraction in the PSD for four oils. It can be seen that the amplitudes decreases approximately linearly as the d_{30} increases.

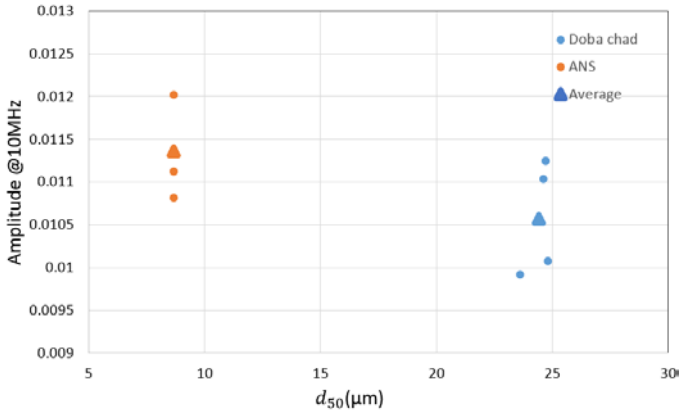

Figure 51. The amplitude of the backscatter coefficient at 10MHz versus the diameter of the scatterer corresponding to 50% volume fraction in the oil droplets distribution (d_{30}) for Doba chad and ANS.

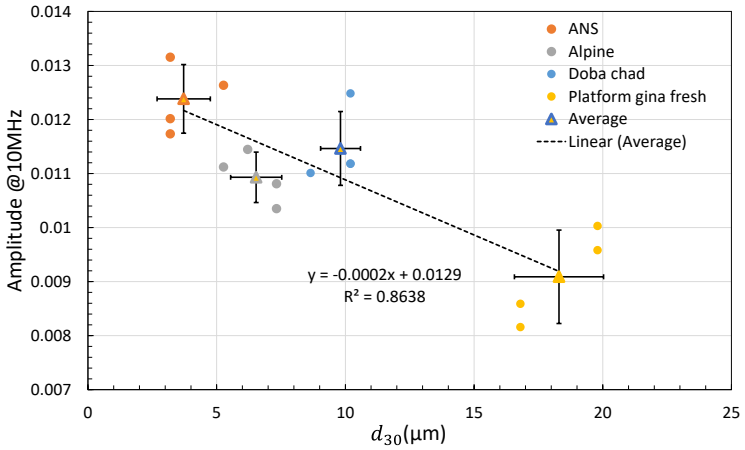

Figure 52. The amplitude of the backscatter coefficient at 10MHz versus the diameters of the scatterers corresponding to 30% volume fraction in the oil droplets distribution (d_{50}) for Doba chad, ANS, Alpine and Platform gina fresh.

Another component of the backscattering that can potentially shed light on the relationship between the droplet size and oil concentration is the frequency response of the acoustic backscattering. Figure 53 and Figure 54 show the frequency response as measured by the power, P, of a power law fit (Af^P) where A is the amplitude of the backscattering, f, is the frequency, and P is the power. The backscattering power coefficient shows little correlation to the dispersant effectiveness for these oils.

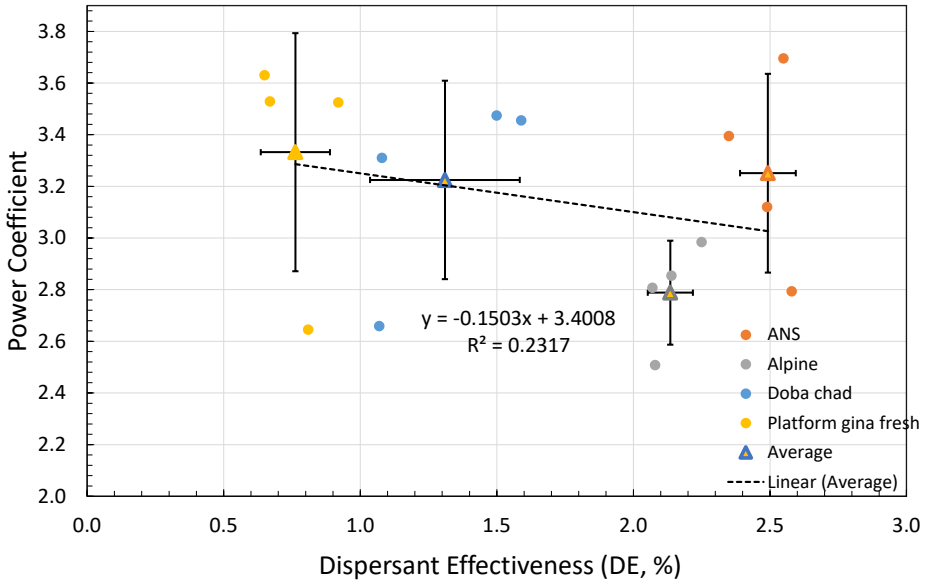

Figure 53. Power coefficient versus the DE for the measurements at 5°C.

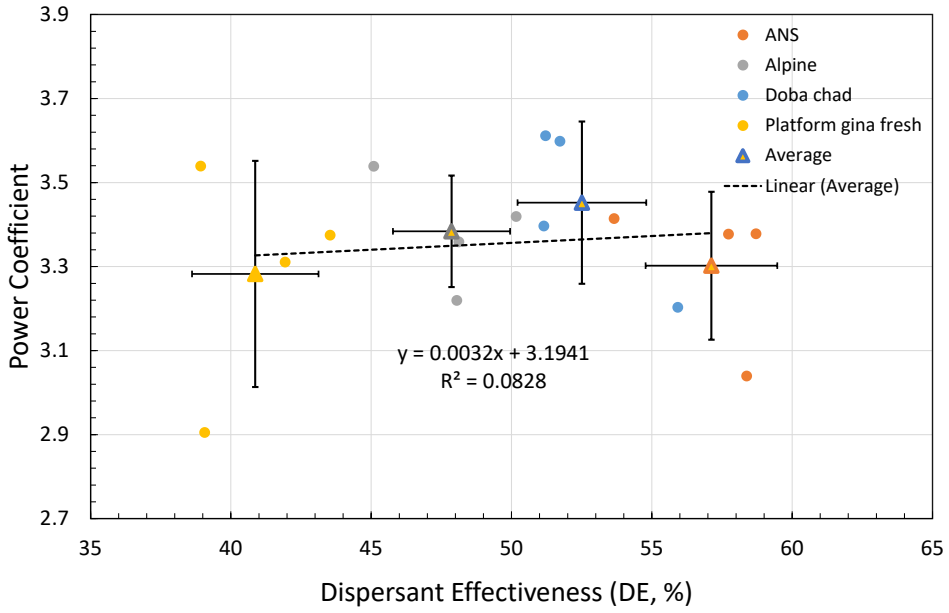

Figure 54. Power coefficient versus the DE for the measurements at 20°C.

6. SUMMARY AND RECOMMENDATIONS

While the dispersant effectiveness is related to oil viscosity, the correlation is not strong, implying there could be other components in the oil that also affect the DE. Out of the two dispersants tested, Finasol generally has a higher DE than Corexit 9500A, and the relationship between viscosity and DE is slightly stronger. The data shows that the correlation between viscosity and DE for Corexit 9500A at 20ºC is significantly stronger than at 5ºC. The opposite relationship is observed for Finasol; the correlation between

viscosity and DE for Corexit 9500A at 20ºC is weaker than at 5ºC. For both dispersants, DE is generally higher at 20ºC, which is expected, because viscosities are lower at higher temperatures.

Since increasing viscosity and decreasing DE do not have a strong correlation, it was thought that there may be a correlation between DE and one of the SARA hydrocarbon groups; however, the data collected in this project does not support that assumption. Asphaltenes show the highest correlation with DE, with R^2 values of 0.4009 and 0.4448 for 20ºC and 5ºC, respectively. Where a higher R^2 value indicated a better fit, with a value of 1 being a perfect fit. Saturates have the weakest correlation with DE with R^2 values of 0.02 and 0.1 for 20ºC and 5ºC, respectively. DE of Finasol correlates with asphaltenes the strongest, with R^2 values of 0.2 and 0.4 for 20ºC and 5ºC, respectively. Saturates are also the most weakly correlated with DE of Finasol, with R^2 values of 0.06 and 0.1 for 20ºC and 5ºC, respectively. Across all four hydrocarbon groups for both dispersants, the correlation was always stronger at 5ºC than 20ºC.

One of the important conclusions that can be drawn from this study is that measurements of DE using the BFT and the LISST produce very different values, with the LISST producing much smaller DE than the BFT. While the trends are the same, the differences are large. While the trends are the same, the differences were as much as a factor of 1.7 at 20°C and a factor of 27 at 5°C. The large differences between the LISST and the BFT could be related to the fact that they are measuring two distinctly different properties of the dispersed oil. In the BFT, the DE is determined based on the amount of oil that is in the water-oil mixture, while in the LISST measurement, the DE is determined as the percentage of oil with droplet sizes below 74.5 μm. The droplet size distributions had a significant number of droplets in the water-oil mixture with sizes above 74.5 μm. In the BFT, all of this oil was measured (even larger droplets) as dispersed, which may be a cause for the disagreement in DE between the two methods.

The acoustic measurements of backscattering amplitude correlated strongly with DE at 20°C with a R^2 value of 0.97, but less so at 5°C with an R^2 value of 0.3. The amplitude of the backscattering also correlated strongly with the d_{30} (the droplet size that corresponds to 30% of the droplets) with an R^2 value of 0.8 at 20°C. The frequency response of the backscattering did not correlate strongly with the DE or average droplet size for the oils measured.

For future measurements, it will be important to correlate DE with additional properties of the oil measured using Gas Chromatography/Mass Spectrometry (GC/MS) tools. It is also recommended that DE measurements be performed at Ohmsett or at another similar meso-scale tank to determine the effects of the larger, more realistic scale and mixing energy to the open water than can be achieved in the tank. As part of that work at Ohmsett, it would be valuable to directly compare LISST results with the results from liquid-liquid extraction followed by UV-Vis measurements on the same samples from the Ohmsett tank to directly study variations between LISST and BFT-type measurements. It would also be useful to perform acoustic measurements and find a theory that can accommodate an arbitrary size distribution.

7. REFERENCES

[1] Alun Lewis and D. Aurand, "Putting Dispersants to Work," *API Publ. 4652A, American Petroleum Institute,* Vols. Washington, D.C., 1997.

[2] M. Fingas and B. Fieldhouse, "Studies of the formation process of water-in-oil emulsions," *Marine Pollution Bulletin,* pp. 47:369-396, 2003.

[3] E. Holder, "Use of the Baffled Flask Test to Evaluate Eight Oil Dispersant Products and to Compare Dispersability of Twenty Three Crude Oils," Master's Thesis - University of Cincinatti, 2011.

[4] V. John, C. Arnosti, J. Field, E. Kujawinski and A. McCormick, "The role of dispersants in oil spill remediation: Fundamental concepts, rationale for use, fate, and transport issues," *Oceanography 29(3),* pp. 108-117, 2016.

[5] Southwest Research Institute, "Dispersant Effectiveness Literature Synthesis," Final Report for BSEE Contract E13PC00010, 2014.

[6] SL Ross Environmental Research, "Comparison of large-scale (Ohmsett) and small-scale dispersant effectiveness test results," Final Report for U.S. Department of the Interior Bureau of Ocean Energy Management, Regulation, and Enforcment, 2011.

[7] Z. Li, K. Lee, T. King, M. Boufadel and A. Venosa, "Assessment of Chemical Dispersant Effectiveness in a Wave Tank under Regular Non-Breaking and Breaking Wave Conditions," *Marine Pollution Bulletin, 56,* pp. 903-912, 2008.

[8] A. Venosa and E. Holder, "Laboratory-Scale Testing of Dispersant Effectiveness of 20 Oils Using the Baffled Flask Test," U.S. Environmental Protection Agency, 2011.

[9] R. Belore, A. Lewis, A. Guarino and J. Mullin, "Dispersant Effectiveness Testing on Viscous, US Outer Continental Shelf Crude Oils and Water-in-Oil Emulsion at Ohmsett," in *International Oil Spill Conference Proceedings,* 2008.

[10] G. Canevari, P. Calcavecchio, K. Beckier, R. Lessard and R. Fiocco, "Key Parameters Affecting the Dispersion of Viscous Oil," in *International Oil Spill Conference Proceedings,* 2001.

[11] B. Mukherjee, J. Turner and B. Wrenn, "Effect of Oil Composition on Chemical Dispersion of Crude Oil," *Environmental Engineering Science,* vol. 28, no. 7, pp. 497 - 506, 2011.

[12] M. Fingas, I. Bier, M. Bobra and S. Callaghan, "Studies on the Physical and Chemical Behaviour of Oil and Dispersant Mixtures," in *The International Oil Spill Conference,* 1991.

[13] G. Blondina, M. Singer, I. Lee, M. Ouano, M. Hodgins, R. Tjeerdema and M. Sowby, "Influence of salinity on petroleum accommodation by dispersants.," *Spill Science & Technology Bulletin 5, 127,* 1999.

[14] "Technical Information Sheet - Global Dispersants Stockpile," Oil Spill Response, October 2017. [Online]. Available: https://www.oilspillresponse.com/globalassets/services/member-response-services/global-dispersant-stockpile/tis-gds-2017-oct-27.pdf. [Accessed 2018].

[15] M. F. Fingas, R. Stoodley and N. Laroche, "Effectiveness Testing of Spill-Treating Agents," *Oil & Chemical Pollution,* vol. 7, pp. 337-348, 1990.

[16] [Online]. Available: http://www.intertek.com/petroleum/testing/sara.

[17] "Environmental Technology Centre," Environment Canada, 2001. [Online]. Available: http://www.etc-cte.ec.gc.ca/databases/Oilproperties/.

[18] V. J. Kaku, M. C. Boufadel and A. D. Venosa, "Evaluation of mixing energy in laboratory flasts used for dispersant effectiveness testing," *Journal of Environmental Engineering,* vol. 132, pp. 93-101, 2006.

[19] F. Grubbs, "Procedures for Detecting Outlying Observations in Samples," *Technometrics,* vol. 11, no. 1, pp. 1-21, 1969.

[20] F. Grubbs, "Sample Criteria for Testing Outlying Observations," in *Annals of Mathematical Statistics*, 1969, pp. 27-58.

[21] W. W. J. S. Hinkle DE, Applied Statistics for the Behavioral Sciences, Boston: Houghton Mifflin, 2003.

8. APPENDIX

The average droplet size distribution, cumulative concentration, and DE over time at 5°C and 20°C for ANS, Alpine, Doba Chad, and Platform Gina Fresh are in the remainder of the appendix.

8.1. LISST MEASUREMENT OF THE DISPERSANT EFFECTIVENESS AT 20°C

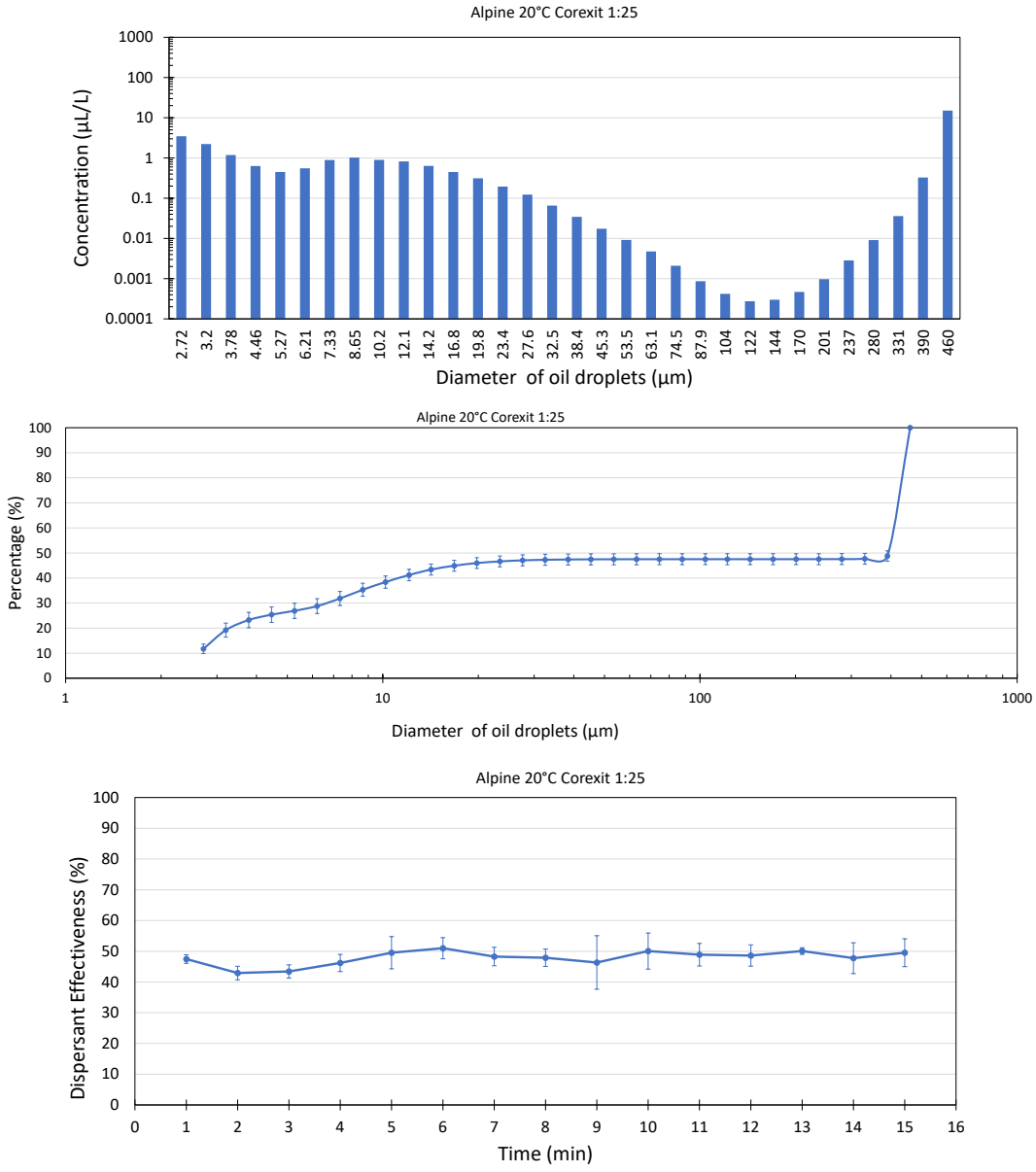

Figure 55. Average droplet size distribution, cumulative concentration, and dispersant effectiveness for Alpine at 20°C for Corexit 9500 with a DOR of 1:25.

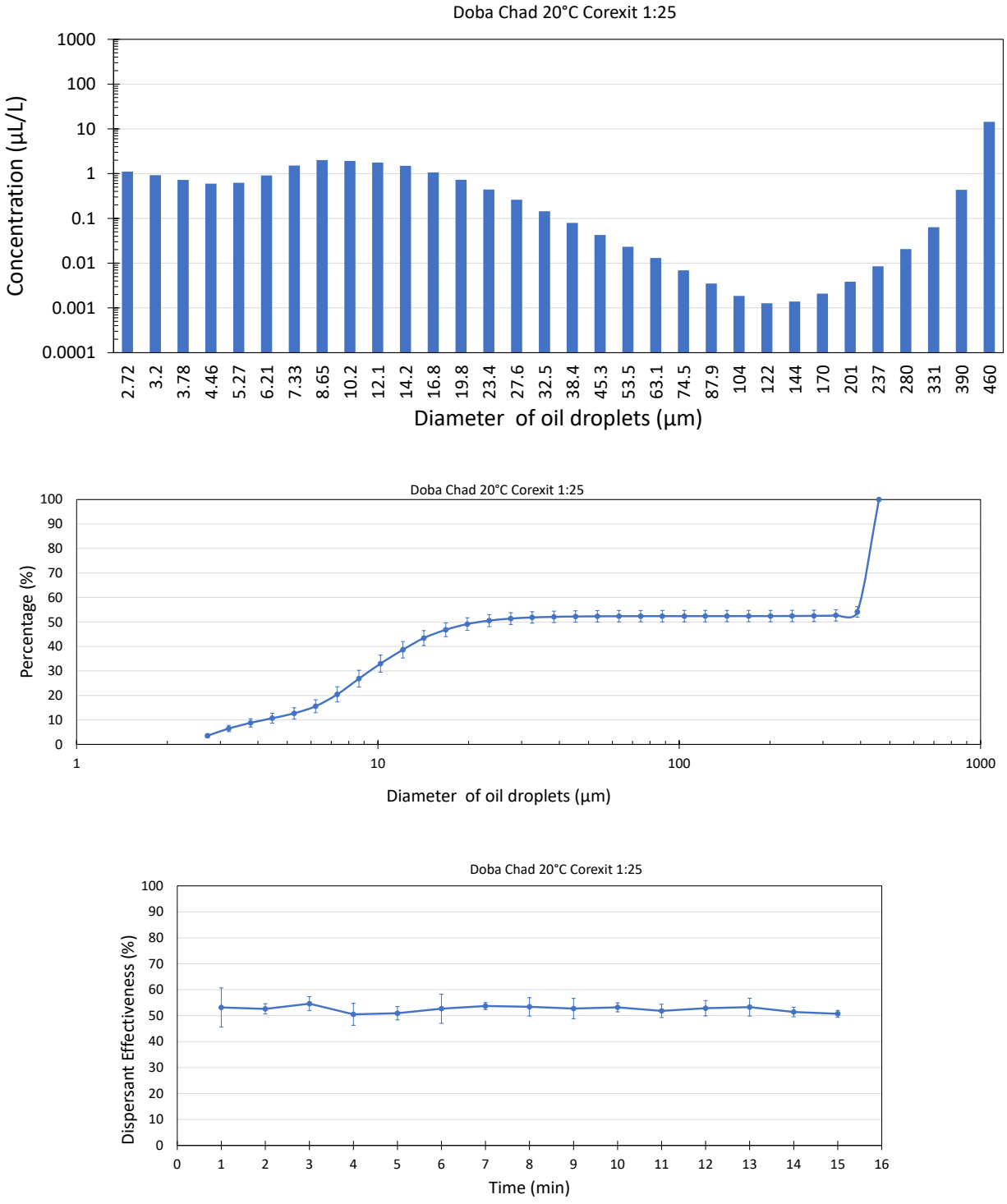

Figure 56. Average droplet size distribution, cumulative concentration, and dispersant effectiveness for Doba Chad at 20°C for Corexit 9500 with a DOR of 1:25.

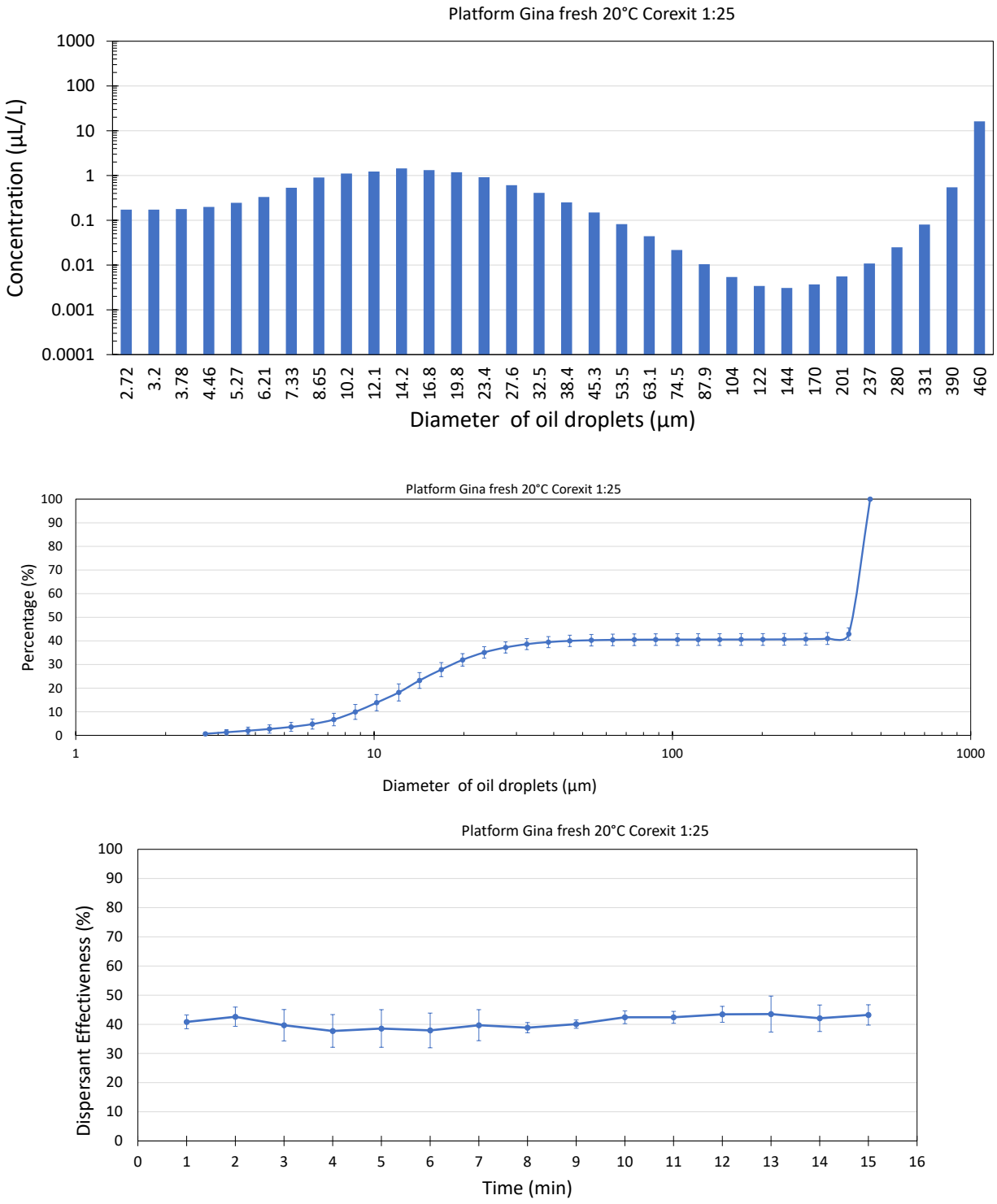

Figure 57. Average droplet size distribution, cumulative concentration, and dispersant effectiveness for Platform Gina fresh at 20°C for Corexit 9500 with a DOR of 1:25.

Table 12. Dispersant effectiveness measured by the LISST at 20°C

Oil	Kinematic Viscosity, cSt	LISST DE	Crude Category by kinematic viscosity
ANS (fresh)	25	55.9%	medium
Alpine	317	47.9%	heavy
Doba Chad	1657	52.5%	heavy
Platform Gina (fresh)	3244	40.9%	heavy

8.2. LISST MEASUREMENT OF THE DISPERSANT EFFECTIVENESS AT 5°C

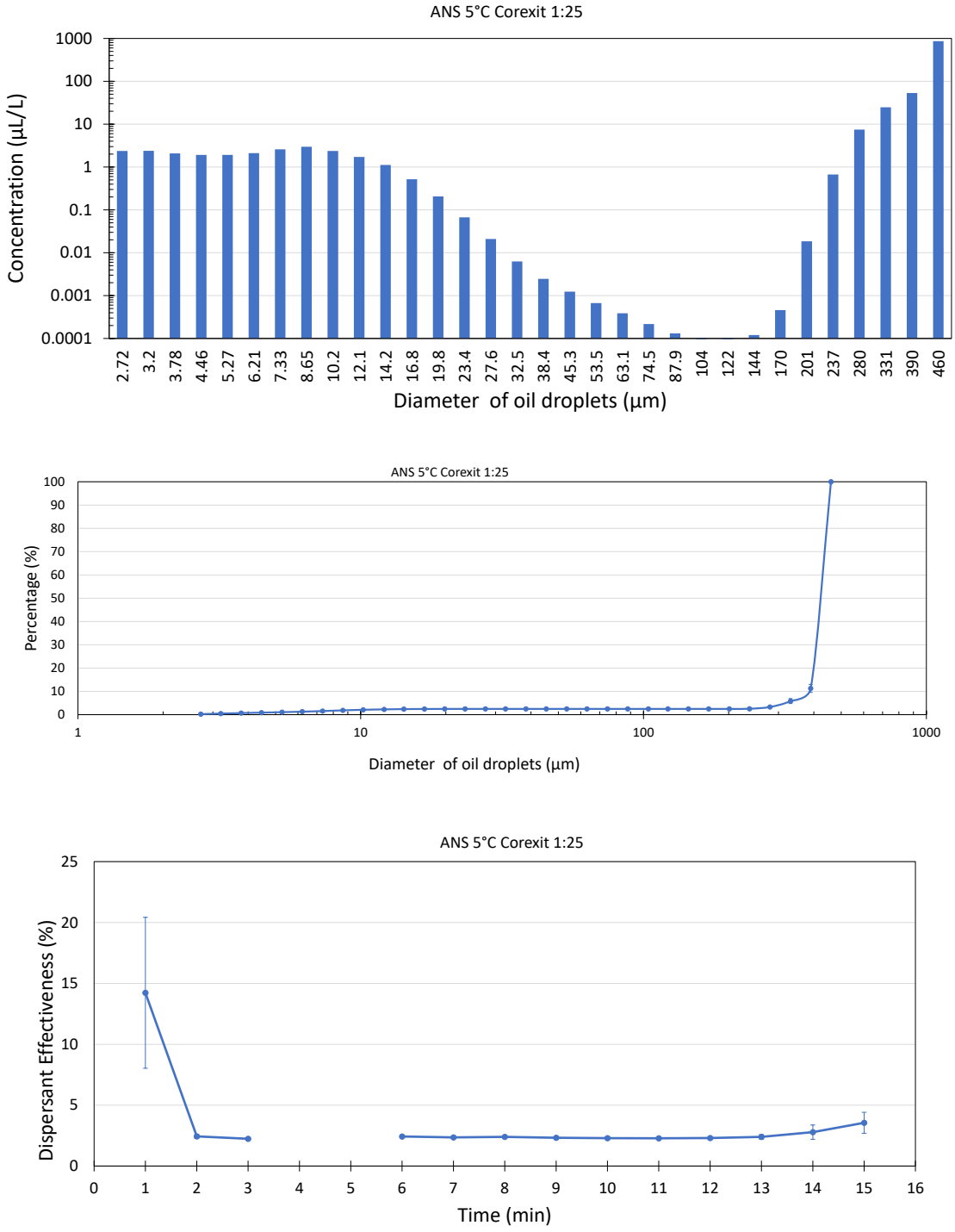

Figure 58. Average droplet size distribution, cumulative concentration, and dispersant effectiveness for ANS at 5°C for Corexit 9500 with a DOR of 1:25.

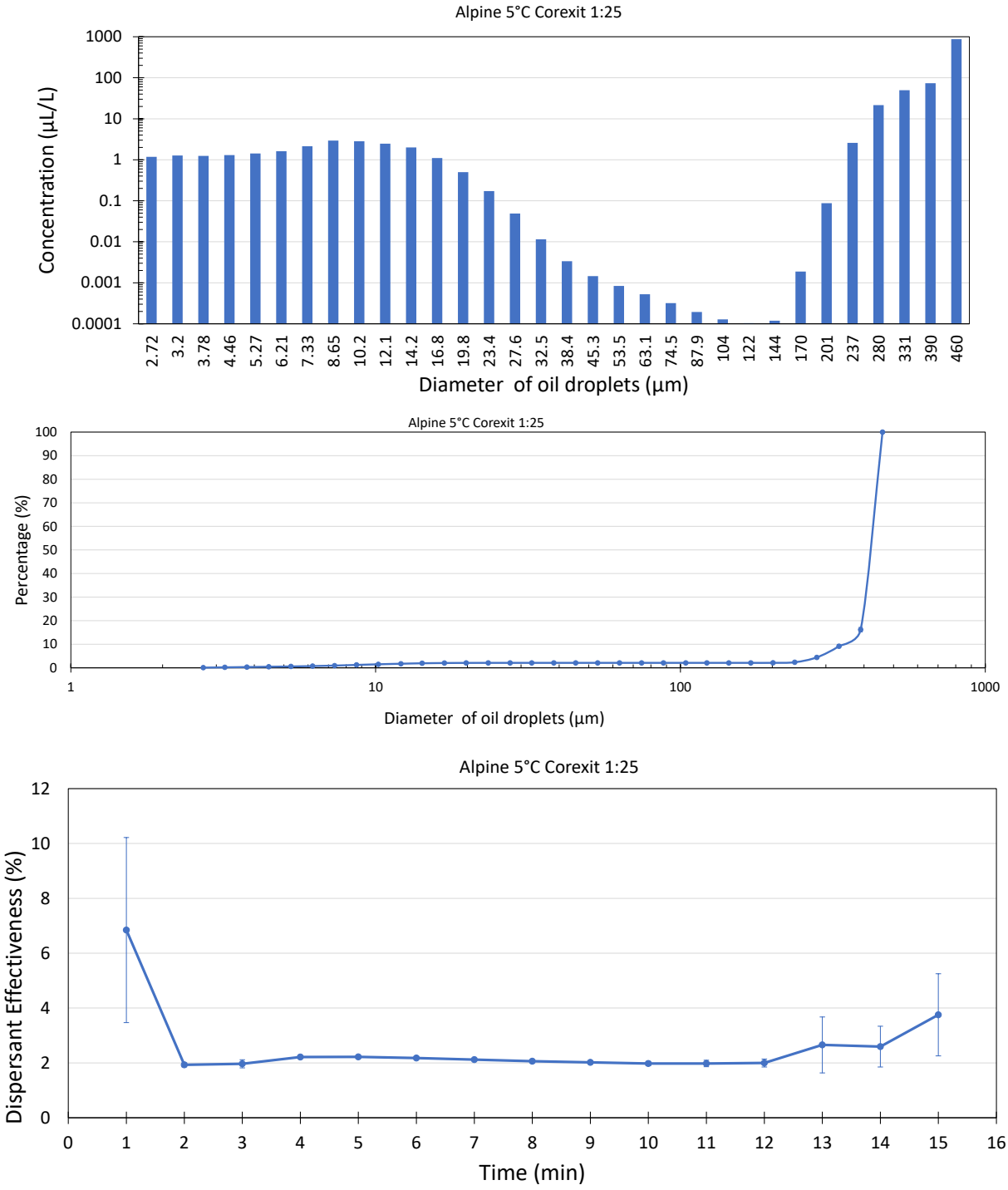

Figure 59. Average droplet size distribution, cumulative concentration, and dispersant effectiveness for Alpine at 5°C for Corexit 9500 with a DOR of 1:25.

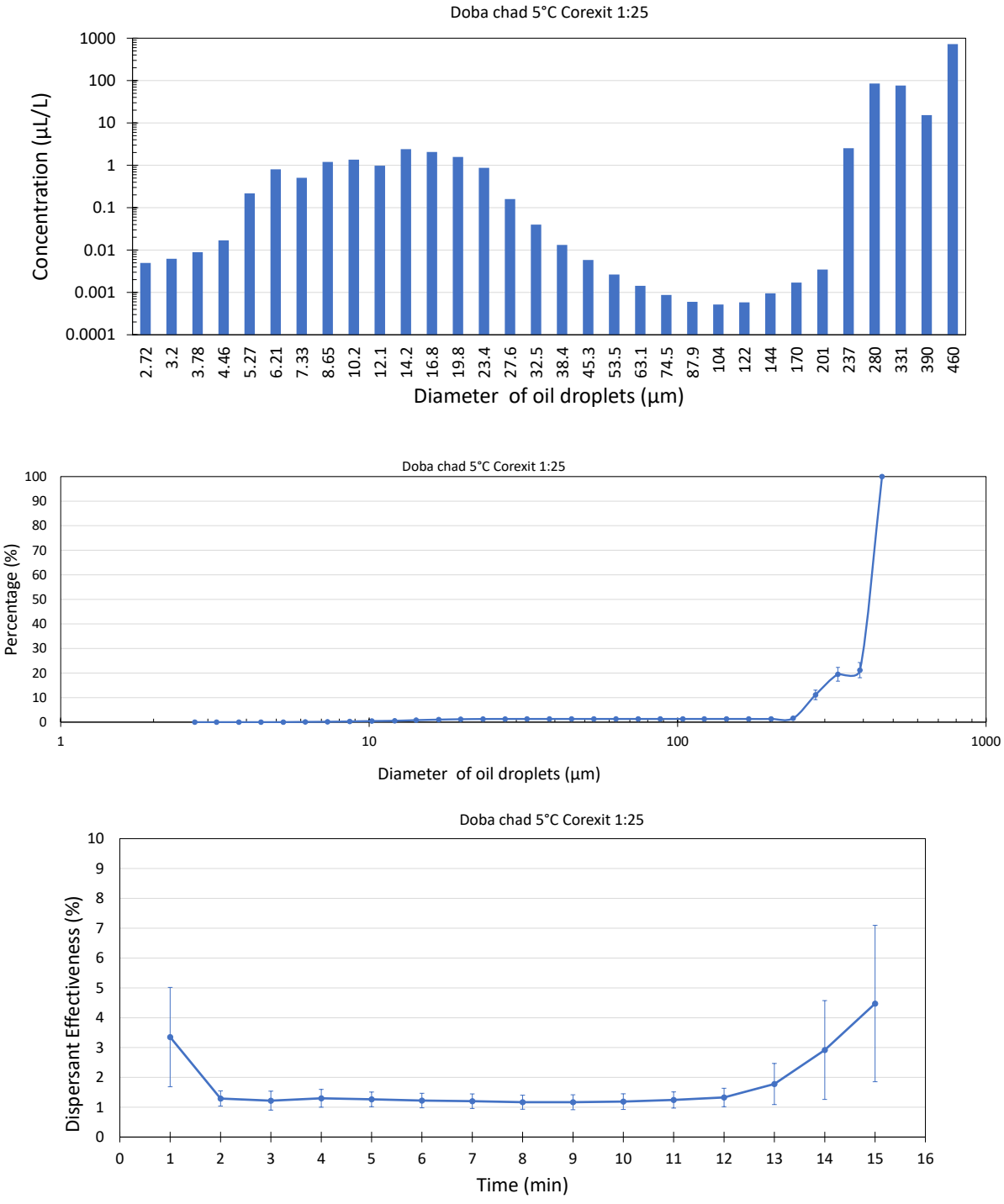

Figure 60. Average droplet size distribution, cumulative concentration, and dispersant effectiveness for Doba Chad at 5°C for Corexit 9500 with a DOR of 1:25.

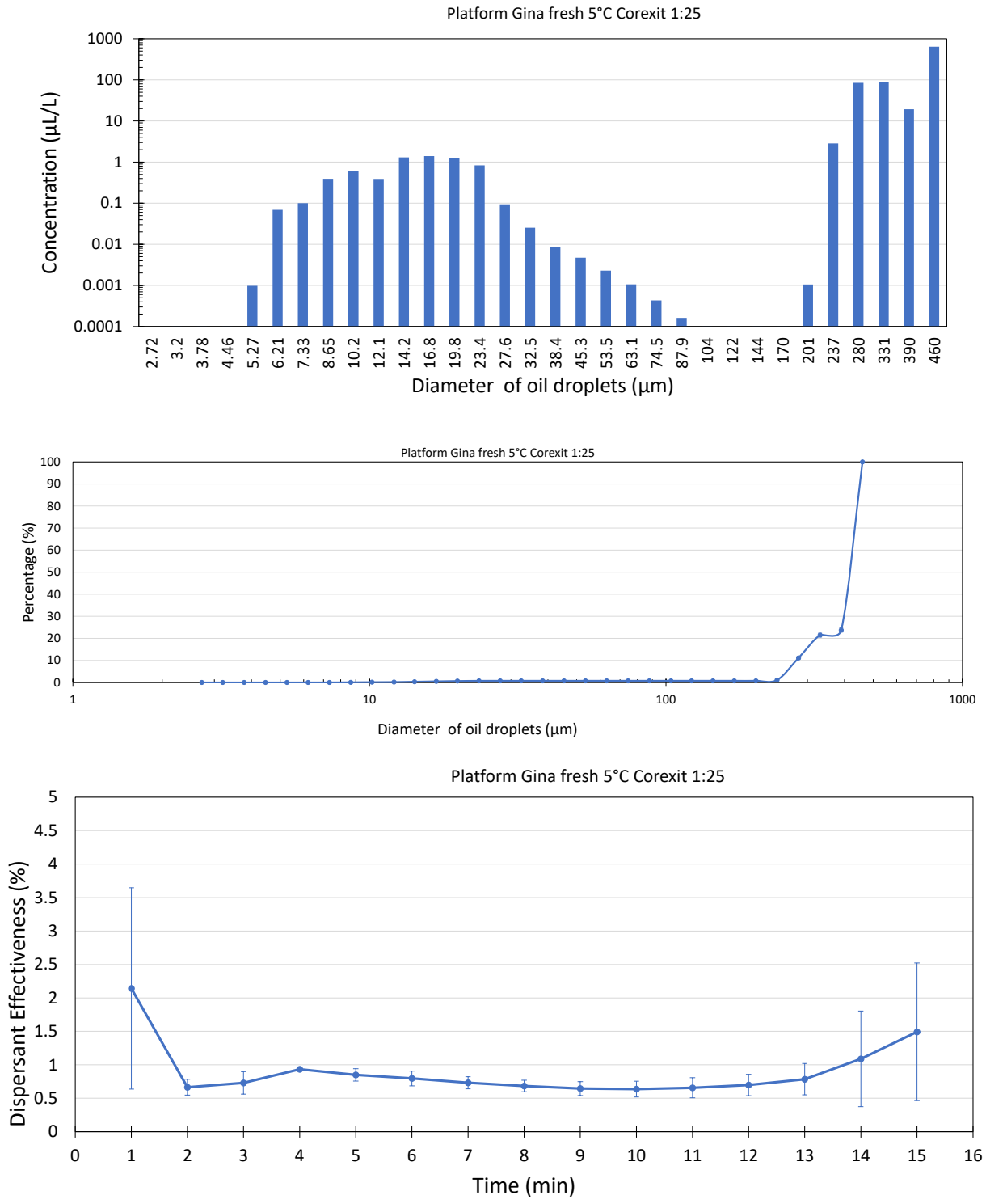

Figure 61. Average droplet size distribution, cumulative concentration, and dispersant effectiveness for Platform Gina Fresh at 5°C for Corexit 9500 with a DOR of 1:25.

Table 13. Dispersant effectiveness measured by the LISST at 5°C

Oil	Kinematic Viscosity, cSt	LISST DE	Crude Category by kinematic viscosity
ANS (fresh)	49	3.4%	medium
Alpine	1368	2.6%	heavy
Doba Chad	8321	1.7%	heavy
Platform Gina (fresh)	15592	0.9%	heavy